SSNET5

Orsay

November 4, 2024

Shapes and rotations of deformed nuclei in a fully quantum many-body view

Takaharu Otsuka

In collaboration with Y. Tsunoda (CNS, Tokyo), N. Shimizu (Tsukuba), Y. Utsuno (JAEA), T. Abe (Keio U.), H. Ueno (Riken), T. Duguet (Saclay)

Supported by “Program for promoting research on the supercomputer Fugaku”, MEXT, Japan (JPMXP1020230411)

Outline

1. Quantum many-body derivation of "rotational energy"

conceptual but practical also

2. Triaxiality and rotational states

3. Vibrational excitations and triaxiality

Rotational states of a microscopic object are relevant to Quantum Computing

→ Proper description/understanding needed

Origin of the J(J+1) rule of rotational excitation energy

conventional description

Ring & Schuck,
The Nuclear Many-Body Problem

classical mechanics

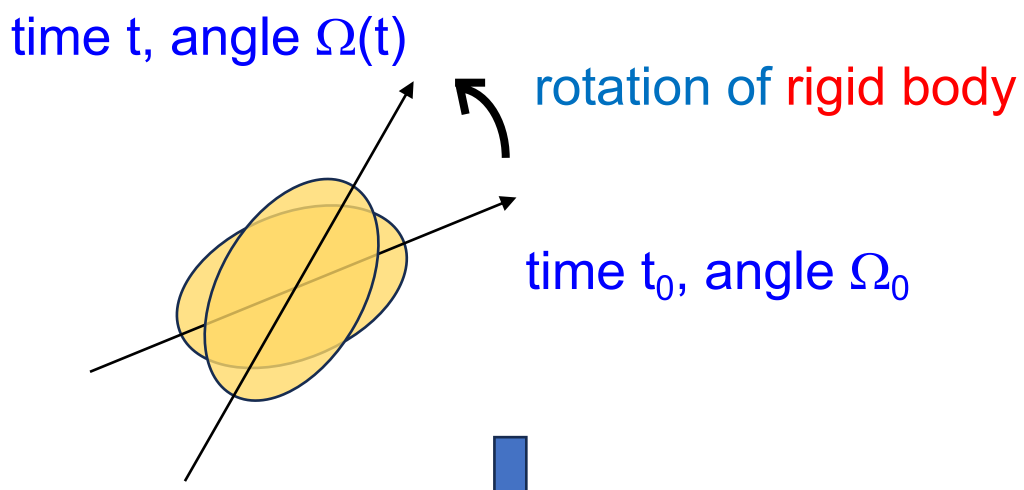

quantization of free rotation of this rigid body
→ eigenstate with angular momentum $\hbar J$

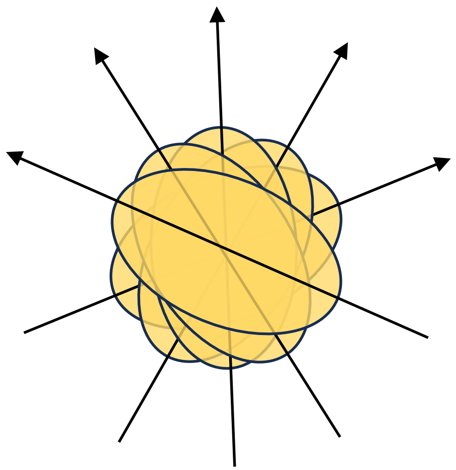

- superposition of states at varying angles
- for axially symmetric shape, J(J+1) rule is suggested
- just kinetic energy of free rotation, no interaction

Bohr Hamiltonian

$$\hat{H}_{\text{coll}} = \frac{-\hbar^2}{2B_2}\left[\beta^{-4}\frac{\partial}{\partial\beta}\left(\beta^4\frac{\partial}{\partial\beta}\right) + \frac{1}{\beta^2 \sin 3\gamma}\frac{\partial}{\partial\gamma}\left(\sin 3\gamma\frac{\partial}{\partial\gamma}\right)\right] + \boxed{\hat{T}_{\text{rot}}} + V(\beta,\gamma).$$

the rotational energy is found to be

$$\hat{T}_{\text{rot}} = \frac{\hat{I}_1^2}{2\mathcal{J}_1} + \frac{\hat{I}_2^2}{2\mathcal{J}_2} + \frac{\hat{I}_3^2}{2\mathcal{J}_3}.$$

Thus, for axially symmetric shapes, the rotational kinetic energy is given by

$$T_{\text{rot}} \propto J(J+1)$$

Nobel Prize 1975

Award ceremony speech

Presentation Speech by professor Sven Johansson of the Royal Academy of Sciences

Translation from the Swedish text

Your Majesties, Your Royal Highnesses, Ladies and Gentlemen

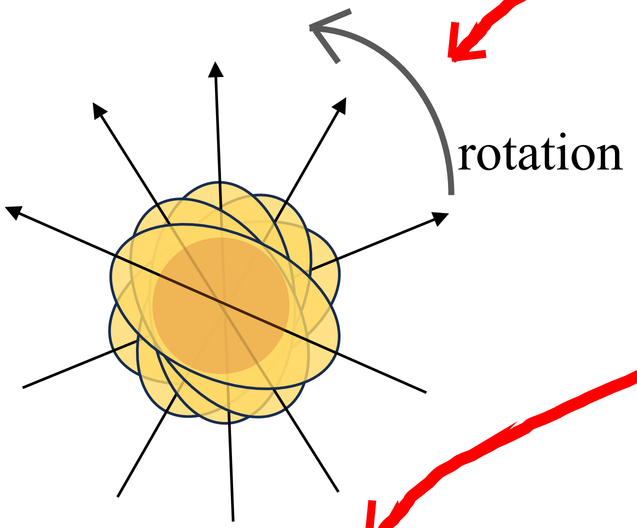

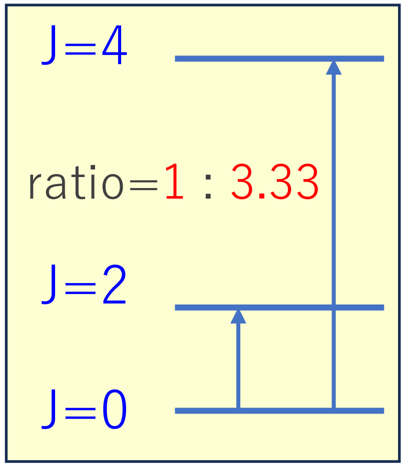

ideal rotor:
$Ex \propto J(J+1)$
rule

These relatively vague ideas were further developed by Bohr in a famous work from 1951, in which he gives a comprehensive study of the coupling of oscillations of the nuclear surface to the motion of the individual nucleons. By analysing the theoretical formula for the kinetic energy of the nucleus, he could predict the different types of collective excitations: vibration, consisting of a periodic change of the shape of the nucleus around a certain mean value, and rotation of the whole nucleus around an axis perpendicular to the symmetry axis. In the latter case, the nucleus does not rotate as a rigid body, but the motion consists of a surface wave propagating around the nucleus.

Up to this point, the progress made had been purely theoretical and the new ideas to a great extent lacked experimental support. The very important comparison with experimental data was done in three papers, written jointly by Aage Bohr and Ben Mottelson and published in the years 1952-53. The most spectacular finding was the discovery that the position of energy levels in certain nuclei could be explained by the assumption that they form a rotational spectrum. The agreement between theory and experiment was so complete that there could be no doubt of the correctness of the theory. This gave stimulus to new theoretical studies, but, above all, to many experiments to verify the theoretical predictions.

……

Drs Bohr, Mottelson and Rainwater,

In your pioneering works you have laid the foundation of a theory of the collective properties of atomic nuclei. This has been an inspiration to an intensive research activity in nuclear structure physics. The further development in this field has in a striking way confirmed the validity and great importance of your fundamental investigations.

Origin of the famous $J(J+1)-K^2$ rule of rotational excitation energy

conventional description

classical mechanics

time t, angle $\Omega(t)$

rotation of rigid body

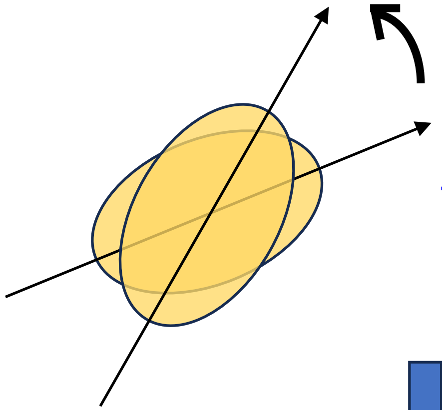

time t_0, angle Ω_0

quantization of free rotation of this rigid body

→ eigenstate with angular momentum $\hbar J$

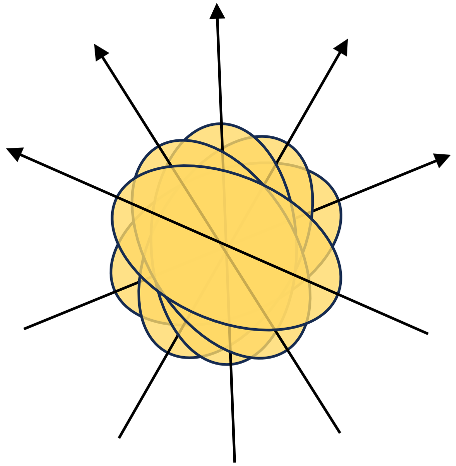

- superposition of states at varying angles
- for axially symmetric shape, $J(J+1)$ rule is suggested
- just kinetic energy, no interaction

view to be discussed

quantum mechanics for many-body system

eigenstate with angular momentum $\hbar J$

- superposition of states at varying angles

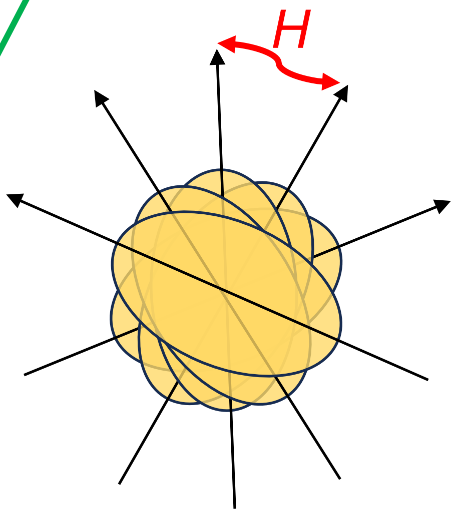

- Hamiltonian H, including interactions, couples states created by orienting the same intrinsic state at different angles
- features are due to specific angle dependence of mixing patterns, which is governed by J

We discuss this view and its consequences in next pages !

Quantum many-body description (derivation) of rotational excitation energy

ϕ_0 : intrinsic state (i.e., state in the body-fixed frame) with K=0

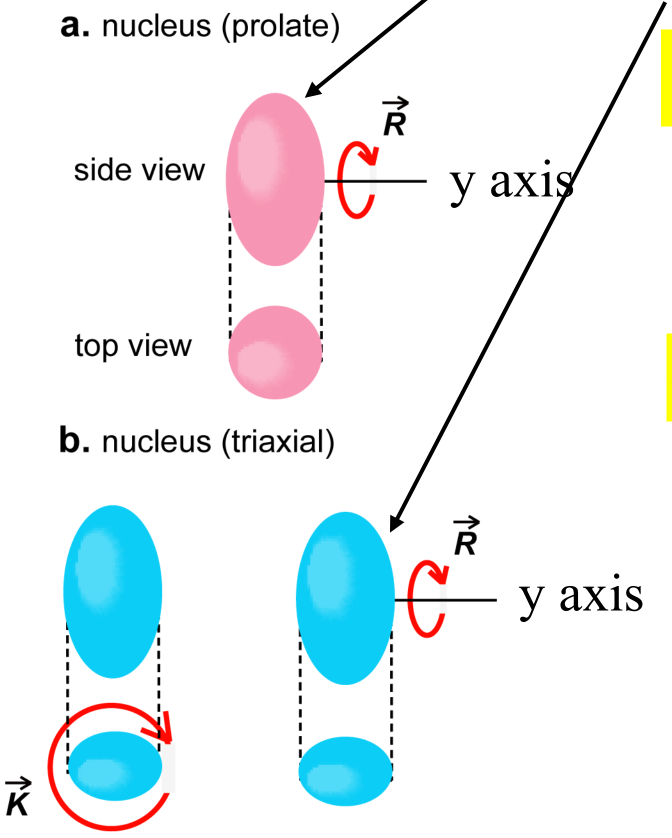

K=0 is assumed
for the time being

symmetry restoration with angular momentum J

state projected onto J $\propto \int_0^{\pi} d\beta \sin\beta \, d^J_{0,0}(\beta) \boxed{e^{i\beta \hat{J}_y} | \phi_0 \rangle}$

rotation about y axis

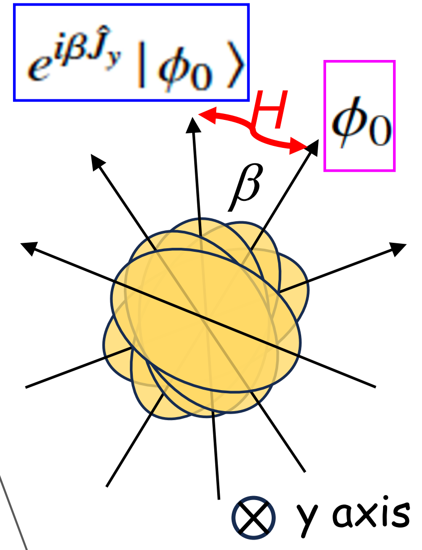

→ energy of the state projected onto J

$$E_J = \frac{2J+1}{2|\mathcal{N}_J|^2} \boxed{\langle \phi_0 |} H \int_0^{\pi} d\beta \sin\beta \; d^J_{0,0}(\beta) \boxed{e^{i\beta \hat{J}_y} | \phi_0 \rangle},$$

$$= \frac{2J+1}{2|\mathcal{N}_J|^2} \int_0^{\pi} d\beta \sin\beta \boxed{d^J_{0,0}(\beta)} \boxed{h_y(\beta)},$$

||

$$\text{energy kernel } h_y(\beta) = \boxed{\langle \phi_0 |} H \boxed{e^{i\beta \hat{J}_y} | \phi_0 \rangle}$$

$$\boxed{d^J_{0,0}(\beta)} = P_J(\cos\beta) \approx 1 + F_J(\cos\beta - 1) + G_J(\cos\beta - 1)^2 + \ldots$$

(see next page)

$$\boxed{d^J_{0,0}(\beta)} = P_J(\cos\beta) \approx 1 + \boxed{F_J}(\cos\beta - 1) + G_J(\cos\beta - 1)^2 + \ldots$$

hierarchy expansion in terms of $(\cos\beta - 1)^k$

a new feature in this analytic aspect

Legendre function satisfies the differential equation:

$$\frac{d}{d(\cos\beta)}\left\{(1-\cos^2\beta)\frac{d}{d(\cos\beta)}P_J(\cos\beta)\right\} + J(J+1)P_J(\cos\beta) = 0.$$

$$\Rightarrow \quad \frac{d}{d(\cos\beta)}P_J(\cos\beta)\Big|_{\beta=0} = \frac{J(J+1)}{2} = \boxed{F_J}$$

$$G_J = \frac{1}{16}\left\{\left(J(J+1)\right)^2 - 2J(J+1)\right\}$$

norm and energy kernels

regions of cos β ~ 1 or -1 are relevant

similar expansion for β ~ -1

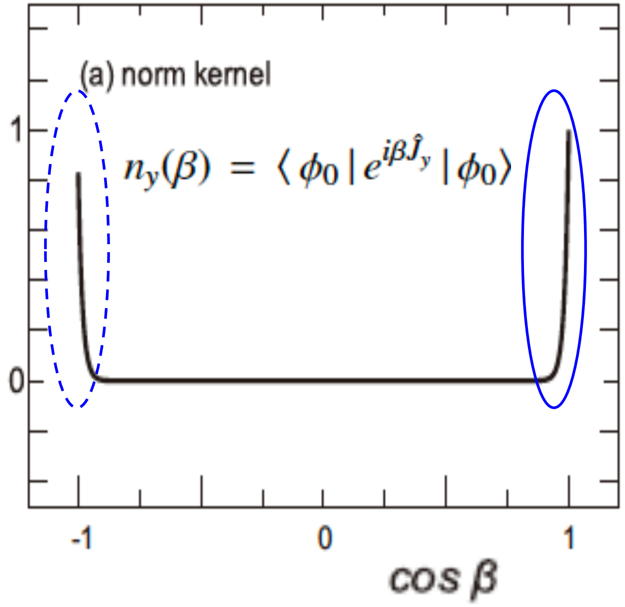

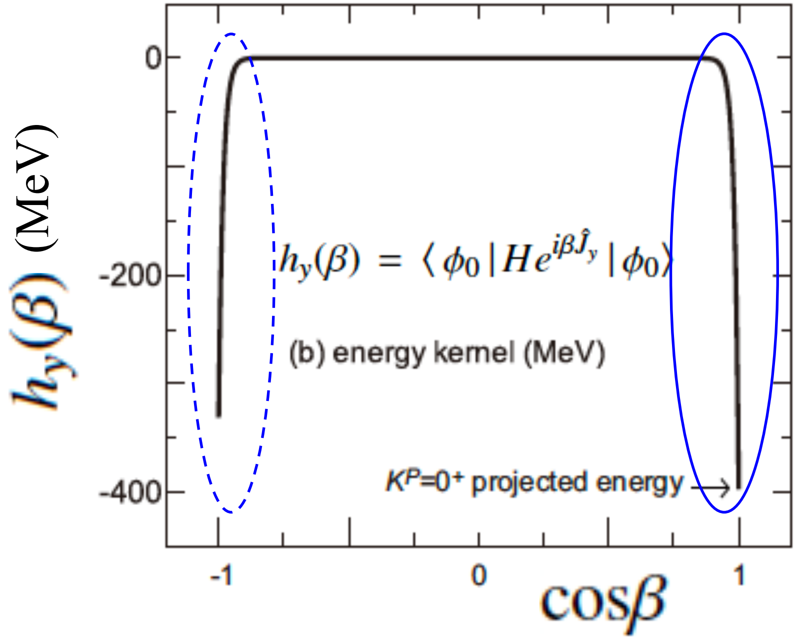

energy for J is given by

$$E_J = \frac{2J+1}{2|N_J|^2}\int_0^{\pi} d\beta \sin\beta\, d^J_{0,0}(\beta)\, h_y(\beta) = \frac{2J+1}{2\boxed{|N_J|^2}}\int_0^{\pi} d\beta \sin\beta \left\{ \boxed{1} + \boxed{F_J}\boxed{(\cos\beta - 1)} + G_J(\cos\beta - 1)^2 + \ldots \right\} h_y(\beta)$$

$$e_0 = \int d(\cos\beta)\, h_y(\beta), \qquad e_1 = \int d(\cos\beta)\, h_y(\beta)\, (\cos\beta - 1)$$

norms are treated similarly

$$\boxed{|N_J|^2} = \frac{2J+1}{2}\int_0^{\pi} d\beta \sin\beta\, d^J_{0,0}(\beta)\, \langle \phi_0 | e^{i\beta \hat{J}_y} | \phi_0 \rangle$$

norm kernel $n_y(\beta) = \langle \phi_0 | e^{i\beta \hat{J}_y} | \phi_0 \rangle$

$$n_0 = \int d(\cos\beta)\, n_y(\beta) \qquad n_1 = \int d(\cos\beta)\, n_y(\beta)\, (\cos\beta - 1)$$

We substitute the first two terms, also for those for the normalization,

$$E_J \approx \frac{e_0 + \boxed{F_J} e_1}{n_0 + \boxed{F_J} n_1} \approx \frac{e_0}{n_0}\left\{ 1 + F_J \frac{e_1}{e_0} - F_J \frac{n_1}{n_0} \right\}$$

for $|e_1| \ll |e_0|$ and $|n_1| \ll |n_0|$

Leading order (LO) & Next to LO (NLO) : substituting $F_J = J(J+1)/2$

$$\boxed{E_J = \frac{e_0}{n_0} + \frac{1}{2} J(J+1) \frac{e_0}{n_0}\left\{ \frac{e_1}{e_0} - \frac{n_1}{n_0} \right\}}$$

deviation ~ 1.5 % to direct projection in the tests so far

LO + NLO + N2LO term,

$$E_J = \frac{e_0 + F_J e_1 + G_J e_2}{n_0 + F_J n_1 + G_J n_2}$$

$$G_J = \frac{1}{16}\left\{\left(J(J+1)\right)^2 - 2J(J+1)\right\}$$

$$E_x^{(2)}(J) = -F_J E_x^{(1)}(J)\frac{n_1}{n_0} + G_J \frac{e_0}{n_0}\left\{\frac{e_2}{e_0} - \frac{n_2}{n_0}\right\}$$

deviation ~ 1.5 % vanishes

generalization: LO + NLO for a finite *K*, by utilizing the hypergeometric function,

$$\boxed{E_{J,K}^{(0+1)} = \frac{\tilde{e}_0}{\tilde{n}_0} + \frac{1}{2}\left\{\boxed{J(J+1) - K^2}\right\}\frac{\tilde{e}_0}{\tilde{n}_0}\left\{\frac{\tilde{e}_1}{\tilde{e}_0} - \frac{\tilde{n}_1}{\tilde{n}_0}\right\}}$$

coefficients are calculated with intrinsic states of assigned K values, differing from those for K=0 in general

K mixing matrix elements can be obtained (not done yet, more complex).

Origin of the famous J(J+1)-K² rule of rotational excitation energy

conventional description

classical mechanics

time t, angle $\Omega(t)$

rotation of rigid body

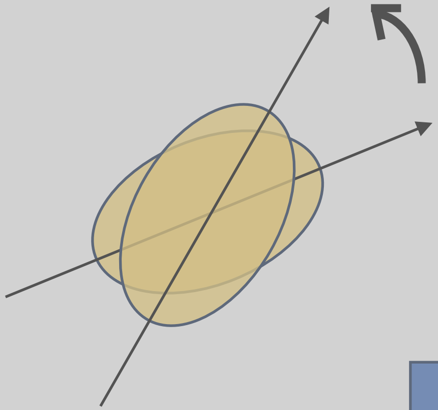

time t_0, angle Ω_0

quantization of free rotation of this rigid body

→ eigenstate with angular momentum $\hbar J$

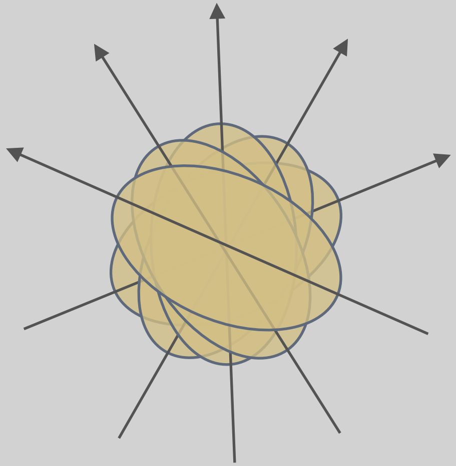

- superposition of states at varying angles
- for axially symmetric shape, J(J+1) rule is suggested
- just kinetic energy, no interaction

present view

quantum mechanics for many-body system

eigenstate with angular momentum $\hbar J$

- superposition of states at varying angles

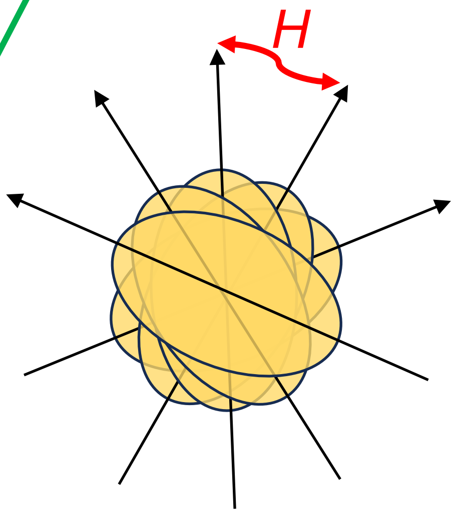

- Hamiltonian *H*, including interactions, couples states at different angles
- resultant excitation energy depicts the J(J+1) – K² rule for strong deformation
- this rule arises from specific angle dependence of mixing patterns, which is governed by *J*
- lower K and J provide more binding energies
- this feature is general and robust

These results are obtained within the quantum many-body framework, without resorting to the quantization of the free rotation of classical object.

The Hamiltonian H stands for a nucleon Hamiltonian which comprises SPEs, *NN* interactions, *3N* interactions, *etc.*

The rotational excitation energy represents a loss of the binding energy provided by this Hamiltonian for each J state, compared to $J=0^+$ energy.

The equations are general and independent of details. They are valid for *ab initio* calculations (such as ^{12}C (R=2.99)) as well as for DFT approaches.

What we need is just a strong deformation, including cluster states.

This simple fact has been missing for seven decades.

This formulation may open a gate for the Nambu-Goldstone Mode; its extension to geometrical symmetry like rotational one has been difficult.

Outline

1. Quantum many-body derivation of "rotational energy"

conceptual but practical also

2. Triaxiality and rotational states

3. Vibrational excitations and triaxiality

Rotational states of a microscopic object are relevant to Quantum Computing

→ Proper description/understanding needed

Types of ellipsoidal shapes of nuclei and comparison to molecules

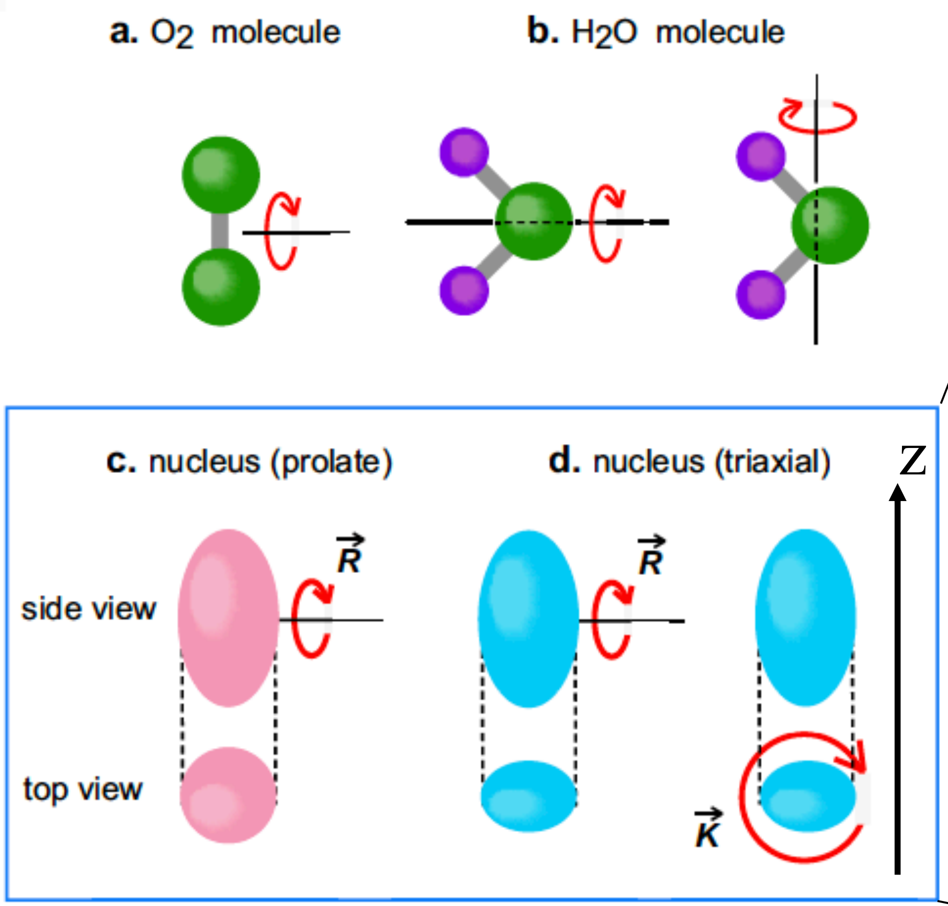

quadrupole moments of the intrinsic state (nuclear state in the body-fixed frame)

$$Q_0 = \langle 2z^2 - x^2 - y^2 \rangle$$

$$Q_2 = \sqrt{3/2}\,\langle x^2 - y^2 \rangle$$

deformation parameters

$$\beta_2^2 \propto (Q_0^2 + 2\,Q_2^2)$$

$$\tan\gamma = \sqrt{2}\,\frac{Q_2}{Q_0}$$

prolate shape $\gamma = 0°$ $\boxed{Q_2 = 0}$

triaxial shape $\gamma \neq 0°$ $\boxed{Q_2 \neq 0}$

(oblate shape $\gamma = 60°$)

The prolate shape has been believed to be dominant over the triaxial shape.

Aage Bohr
Novel Prize Lecture
(1975)

Aage N. Bohr, 1922-2009
Nobel Foundation archive

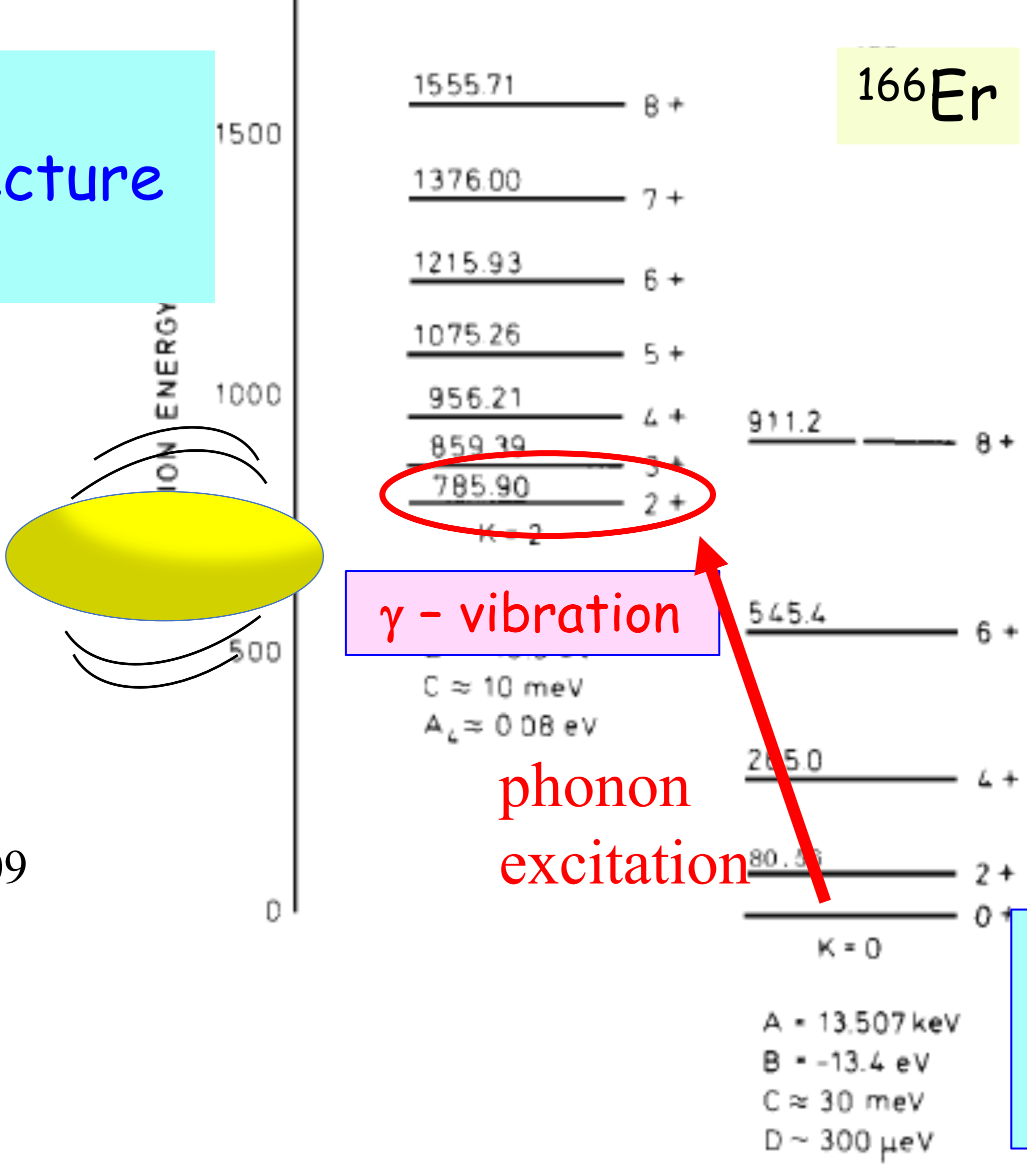

γ - vibration

phonon
excitation

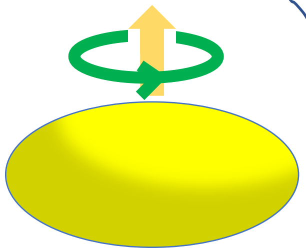

Axially symmetric
prolate ellipsoid
(equilibrium)

Fig. 9. Rotational bands in ^{166}Er. The figure is from (35) and is based on the experimental data by Reich and Cline (75). The bands are labelled by the component K of the total angular momentum with respect to the symmetry axis. The K = 2 band appears to represent the excitation of a mode of quadrupole vibrations involving deviations from axial symmetry in the nuclear shape.

A case of the textbook example:
原子核 by M. Nogami

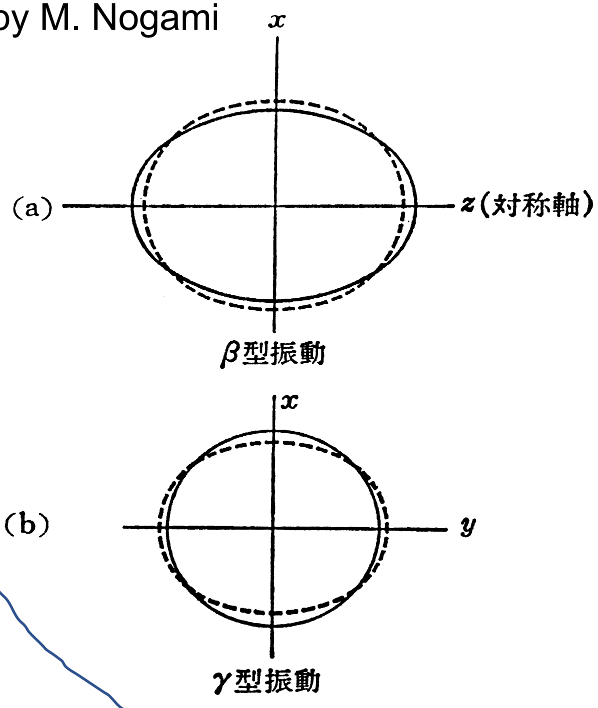

5 – 16 図

also emphasized in
A. Bohr and B. R. Mottelson,
Nuclear Structure II
(1975, Benjamin, New York)

Revisit with Monte Carlo Shell Model

Effective interaction: G-matrix* + V_{MU}

* Brown, PRL 85, 5300 (2000)

Nucleons are excited fully within this model space (no truncation)

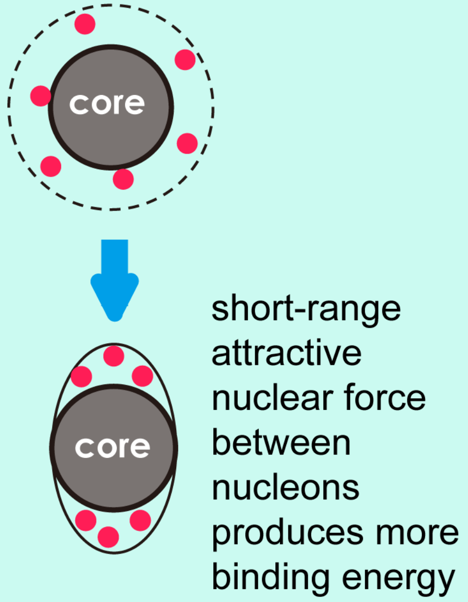

We performed Monte Carlo Shell Model (MCSM) calculations, where the largest case corresponds to the diagonalization of 3.9×10^{31} dimension matrix.

Its recent extension, Quasiparticle Vacua Shell Model (QVSM)* is used, in order to incorporate pairing and deformation effects on an equal footing.

*Shimizu *et al*, PRC 103, 014312 (2021)

+ HFB (number VAP, J VBP) + GCM for γ

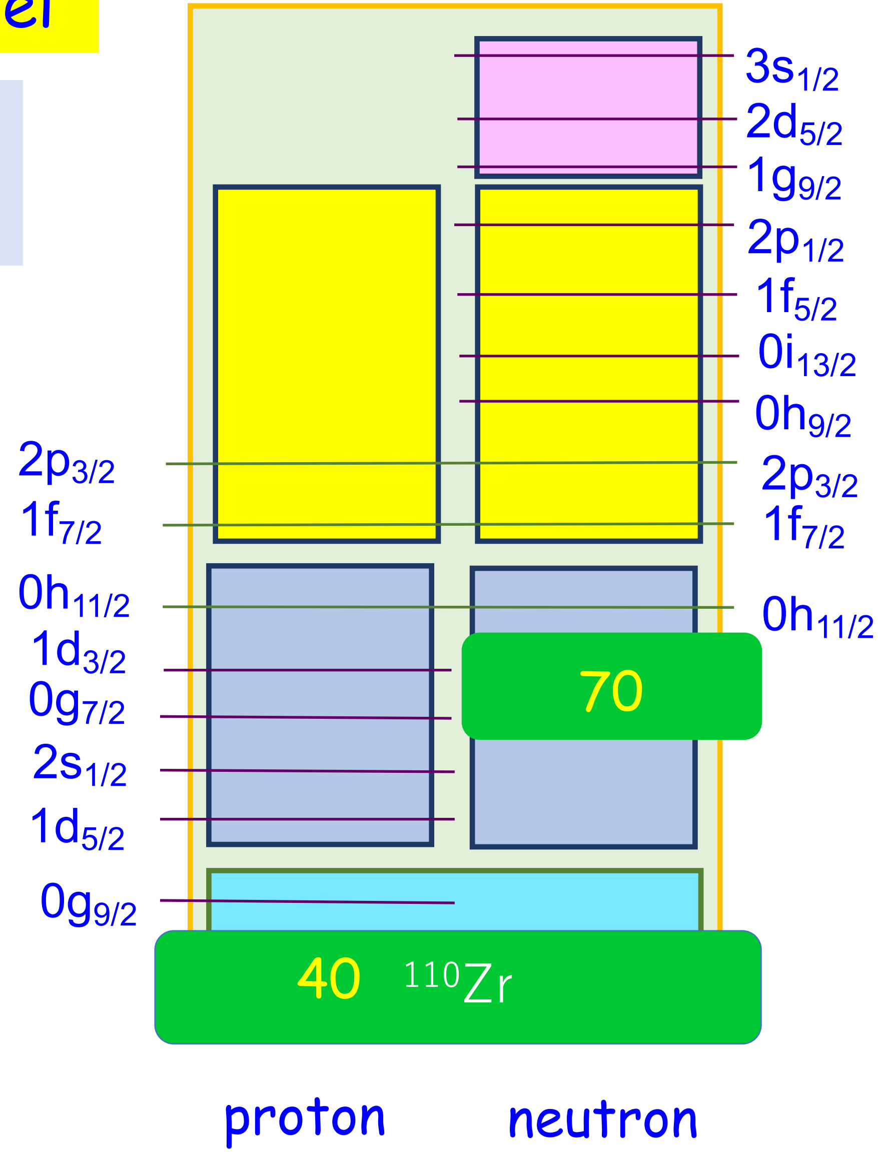

V_{MU} : same interaction for the description of shell evolution in exotic nuclei

Aage Bohr's picture

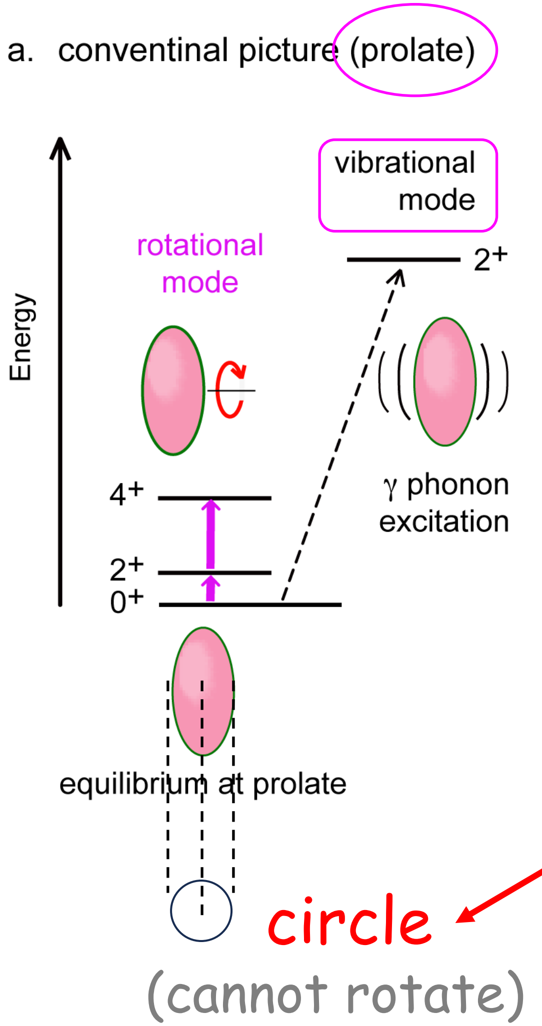

Our picture

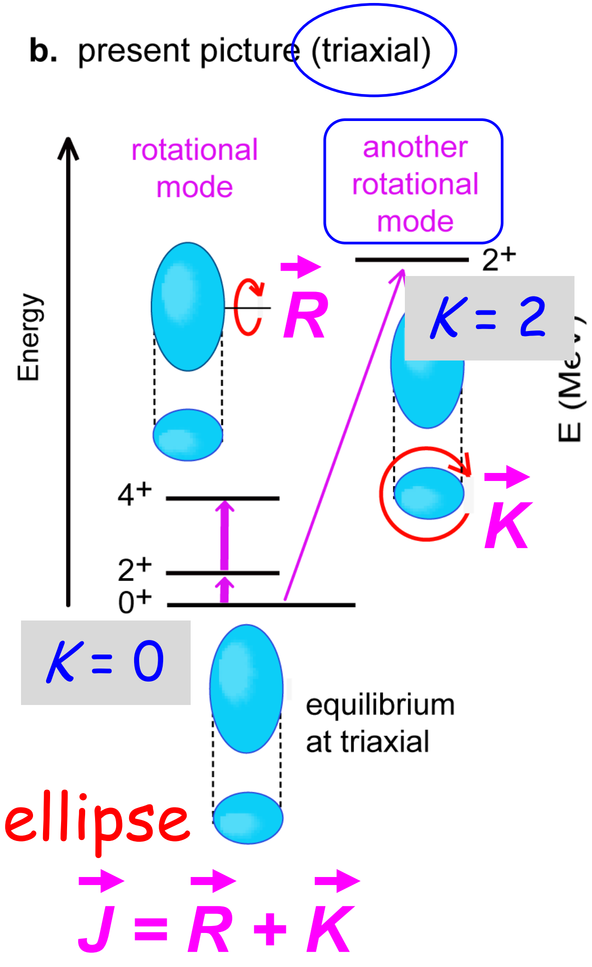

Result of MCSM calculation (QVSM)

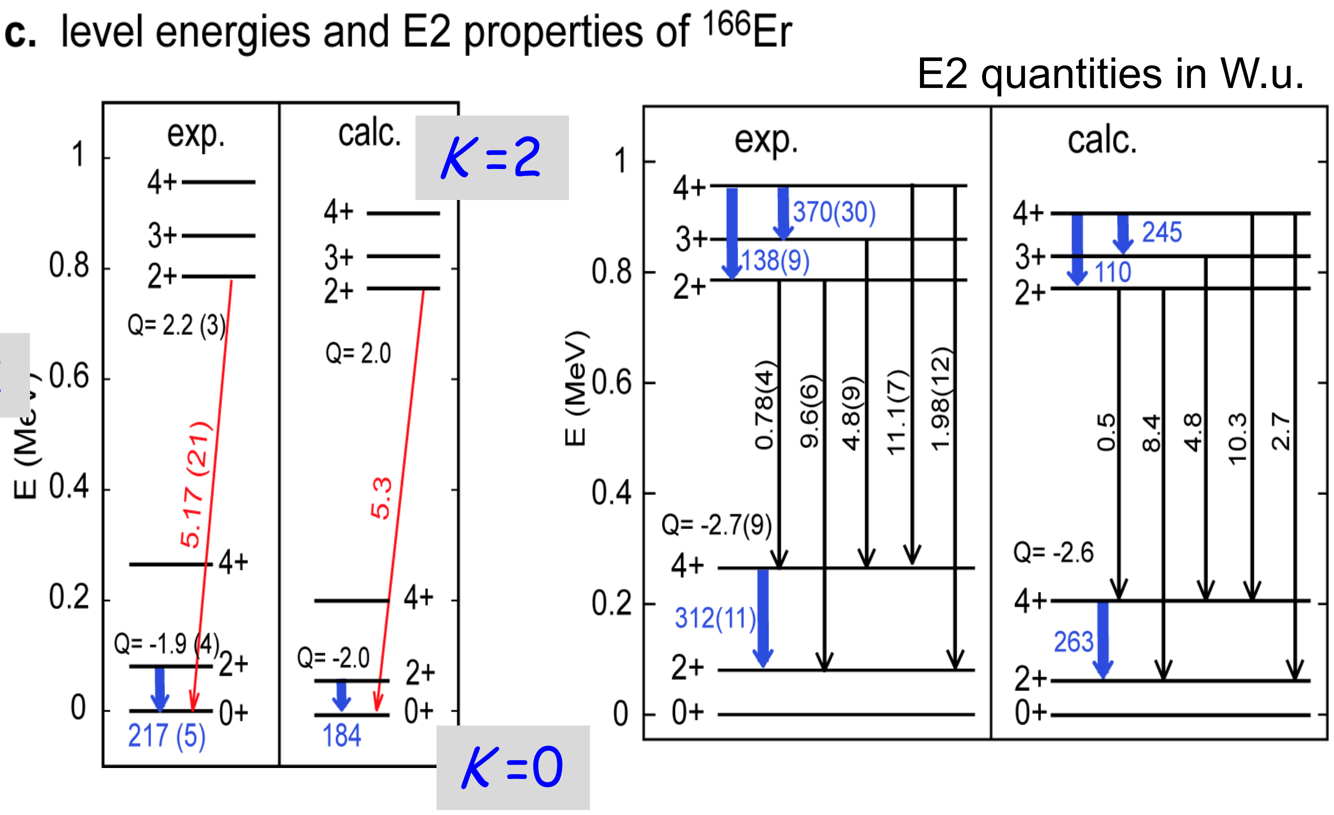

In the present case, the mixing between K=0 and K=2 states is small, and can be neglected.

The MCSM result points to a triaxial shape with axis ratio, 1.00 : 1.06 : 1.35, through its T-plot analysis (see next pages).
No hint of vibrational excitation.

Shape variables and their visualization for the ground and lowest states of ^{166}Er

T-plot: Distribution of basis vectors

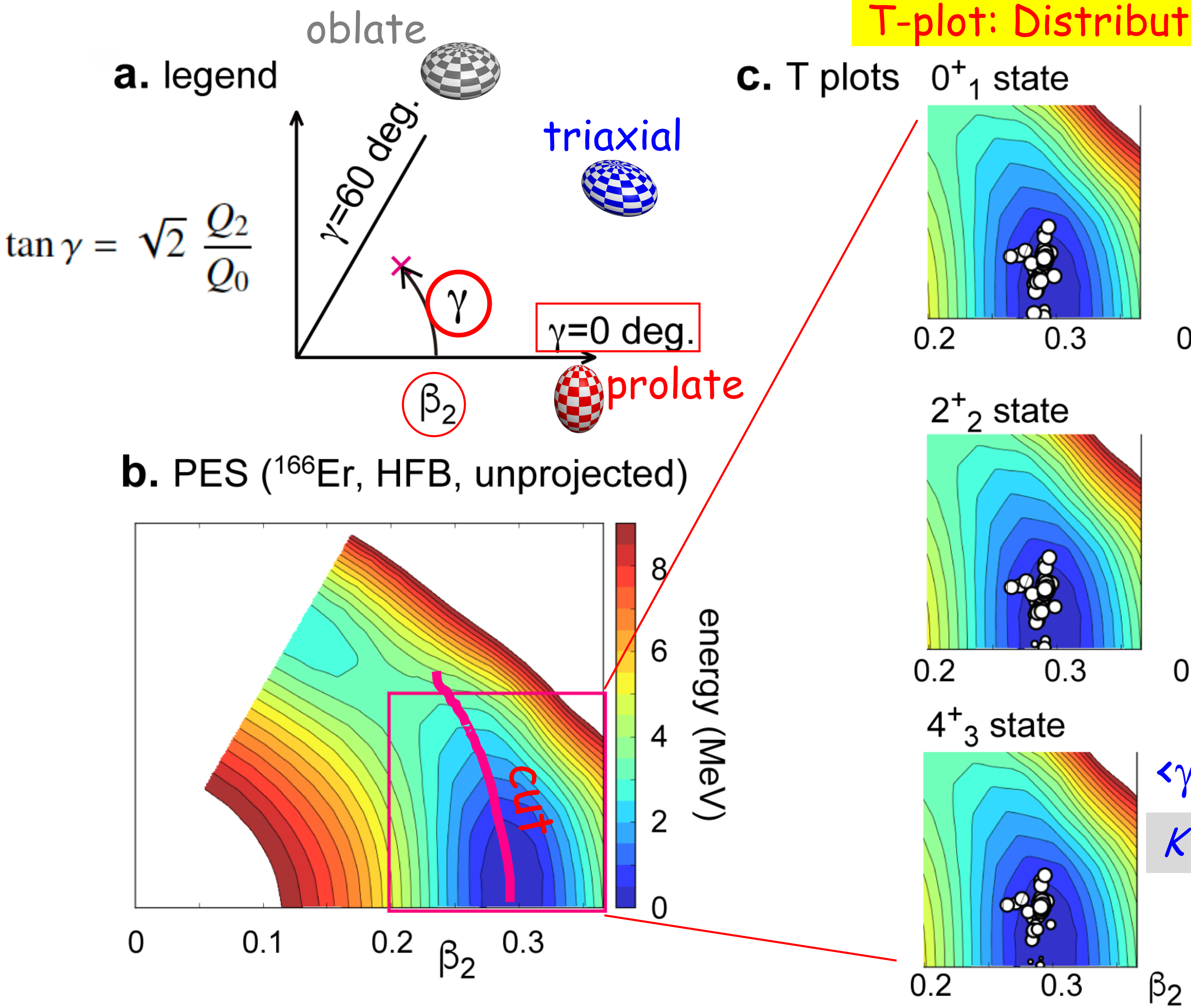

triaxial with $\langle\gamma\rangle$ = 8.4 deg

K = 0

triaxial with $\langle\gamma\rangle$ = 9.1 deg

K = 2

$\langle\gamma\rangle$ = 9.5 deg

K = 4

Similar result from Kumar invariant
$\langle\gamma\rangle \sim$ 9.2 deg, $\langle\beta_2\rangle \sim$ 0.30

Two major origins of triaxiality

1. Restoration of broken rotational symmetry in the intrinsic state

2. Specific components of NN interaction

   … effects seen in unprojected PES

   independently of the symmetry restoration

Broken rotational symmetry in the xy plane as represented by the ellipse.

This symmetry is restored by the projection onto a good *K* value

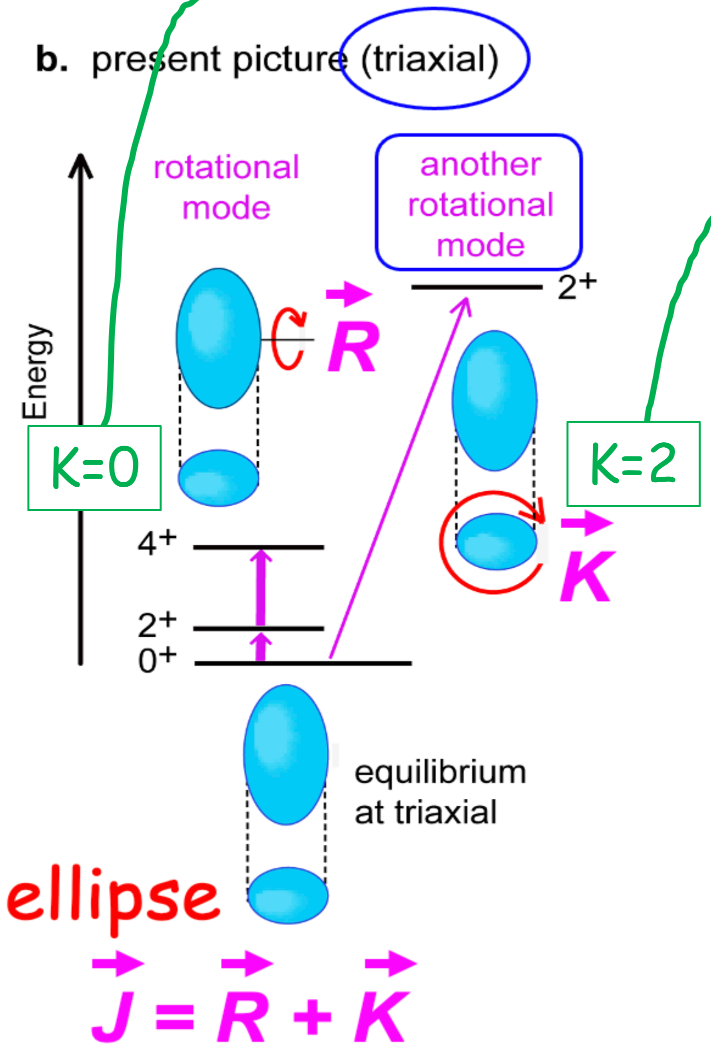

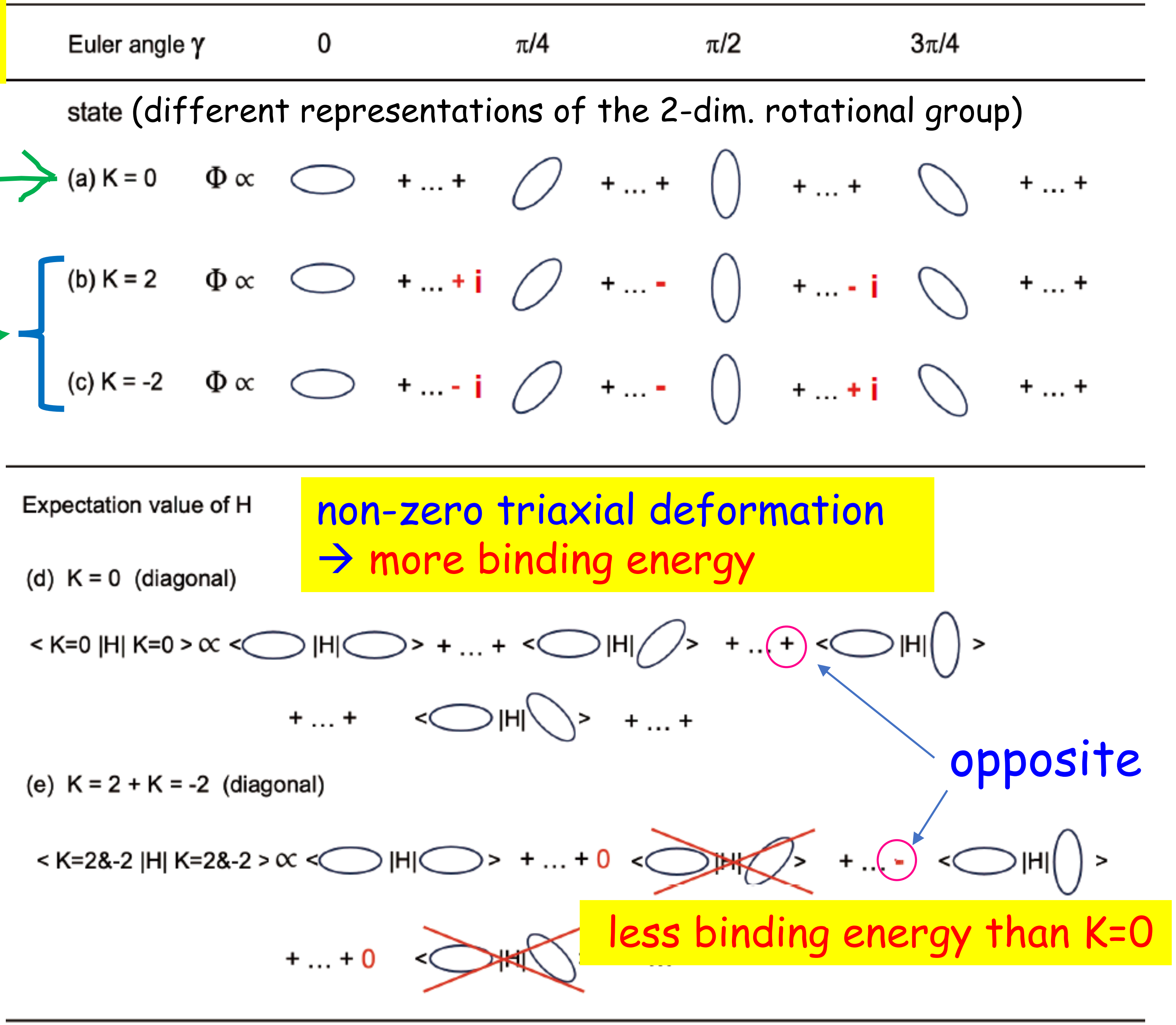

Unprojected and projected energies relative to γ=0 value as a function of γ

Along the cut (β = 0.3) in the PES

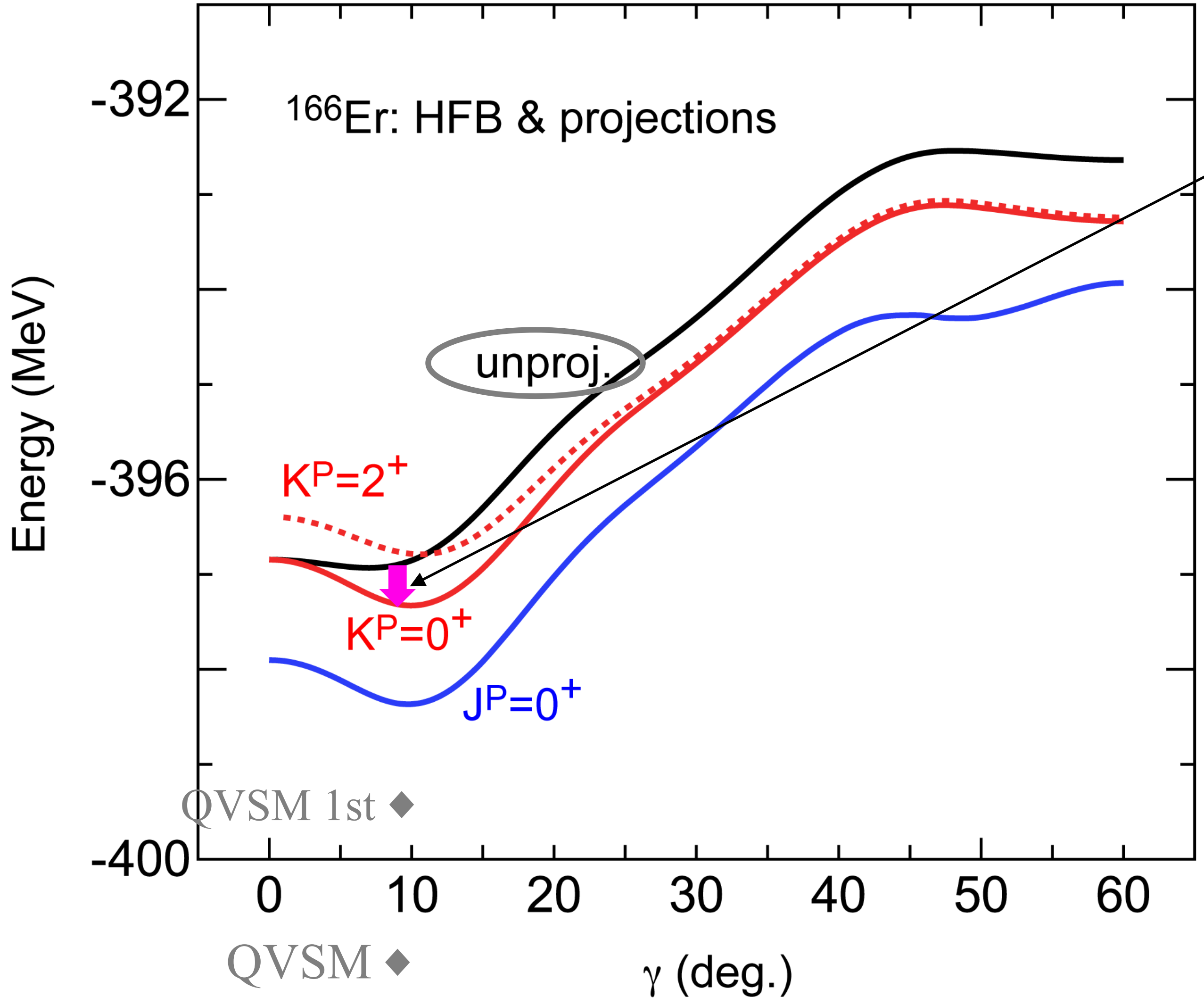

HFB with good particle number for the same Hamiltonian

lowering of K=0$^+$ projected state

the triaxiality gives more binding energy to K=0$^+$

triaxiality is not a fluctuation but a mean effect

A non-trivial feature:

The flat bottom of the unprojected PES is one of the crucial factors for yielding the distinct triaxial minimum after the projections onto K=0$^+$ (or 2$^+$).

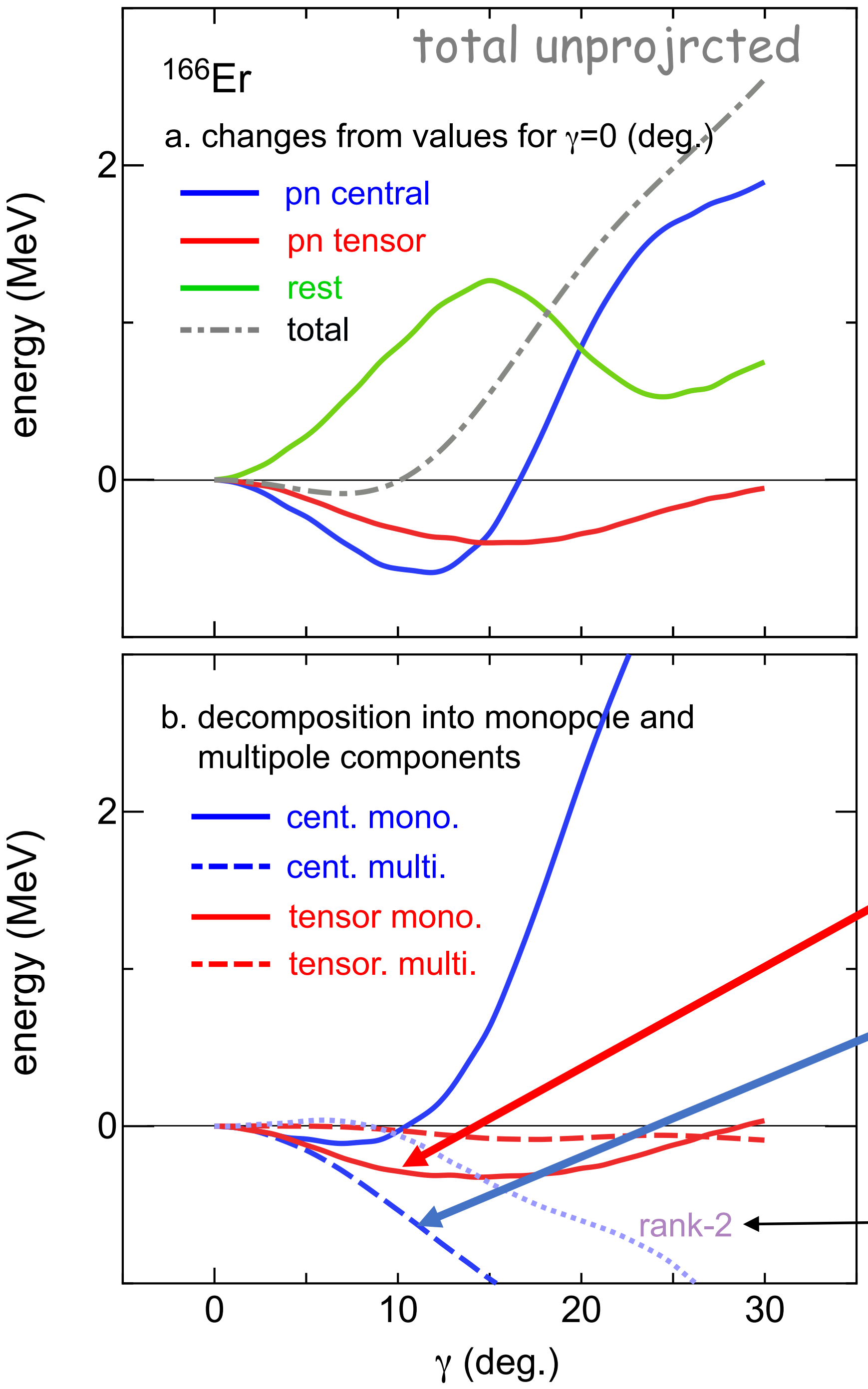

An anatomy of the energy of unprojected state relative to γ=0 value as a function of γ

decomposition into individual effects of pn central, pn tensor and rest components

Further decomposition into monopole and multipole components → major players identified

tensor monopole int.
&
central high-rank multipole (hexadecupole) int.

quadrupole int. gives more binding energy to more deformed states, but is neutral for triaxiality, because $\beta_2^2 \propto Q_0^2 + 2Q_2^2 \sim (\hat{Q}\,\hat{Q})$

Two origins and two appearances of triaxiality in deformed heavy nuclei

1. Basic (modest) triaxiality due to symmetry restoration with K

If only this works, deformation parameter γ is typically up to 5 degrees.
This occurs in most (perhaps all) deformed nuclei.

2. Prominent triaxiality mainly due to
monopole part of pn tensor force
and/or
hexadecupole (multipole) part of pn central force

Both cases involve high-j orbitals, like $g_{9/2,7/2}$, $h_{11/2,9/2}$, $i_{13/2,11/2}$, *etc.*

Deformation parameter γ ranges from 6 to 14 degrees (or more).
This occurs in selected heavy deformed nuclei (~half ?).

Systematic behaviors by MCSM (QVSM)

Levels, B(E2)'s and Q-moments

γ ~ Multiple CoulEx value

B(E2; $0^+_1 \to 2^+_{gamma}$)

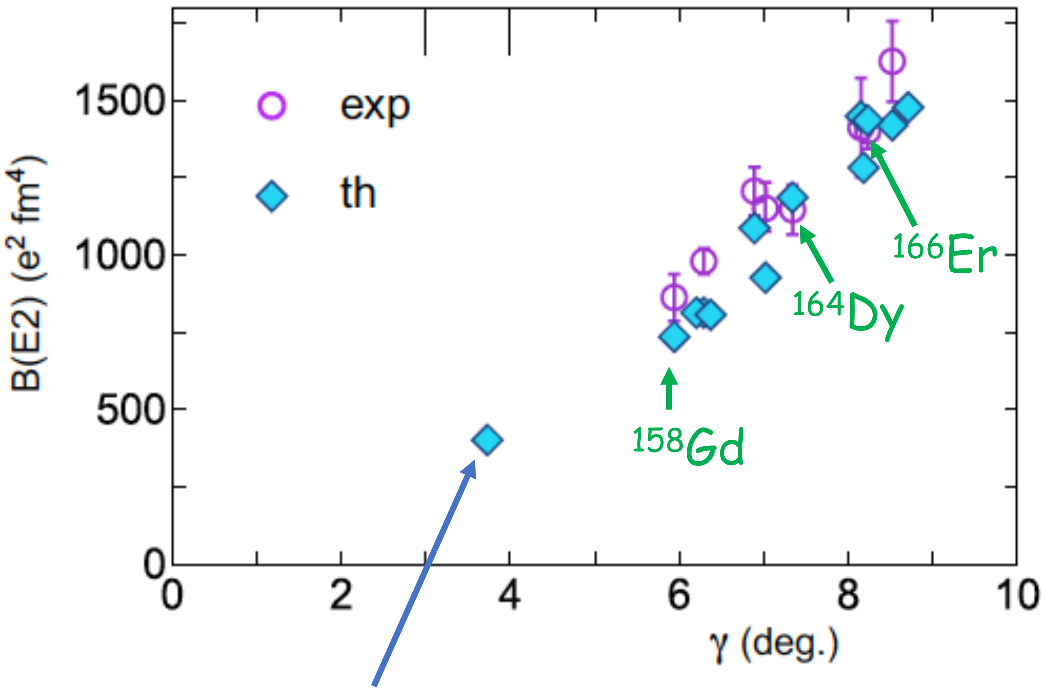

B(E2) from 2^+ at Ex~2.7 MeV of ^{154}Sm

γ = 3.7 deg (^{154}Sm)

supported by a recent GDR (Kleemann *et al.*, 2024) experiment (γ = 5.0 +- 1.4 deg)

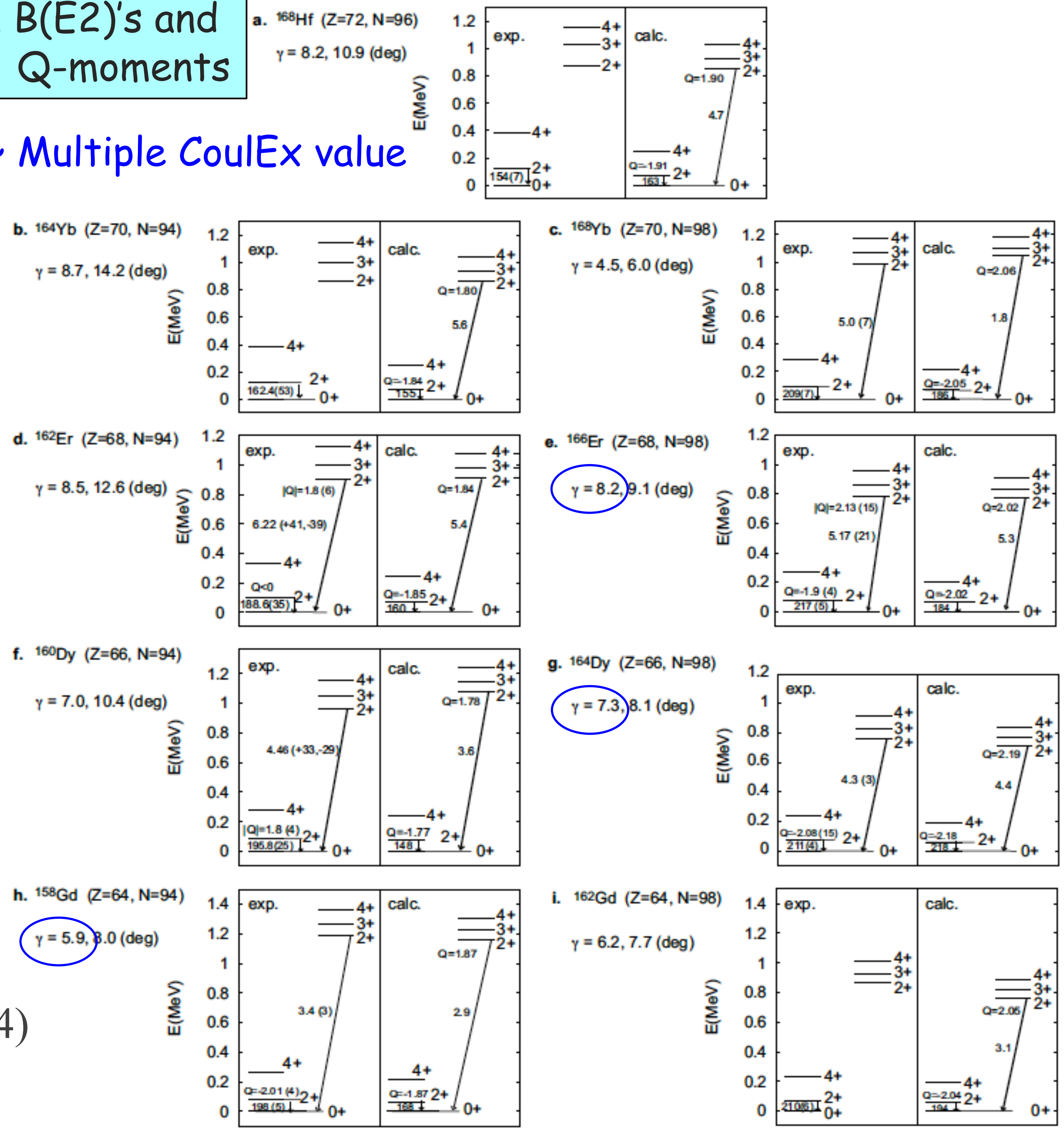

Appearance of prominent triaxial shapes

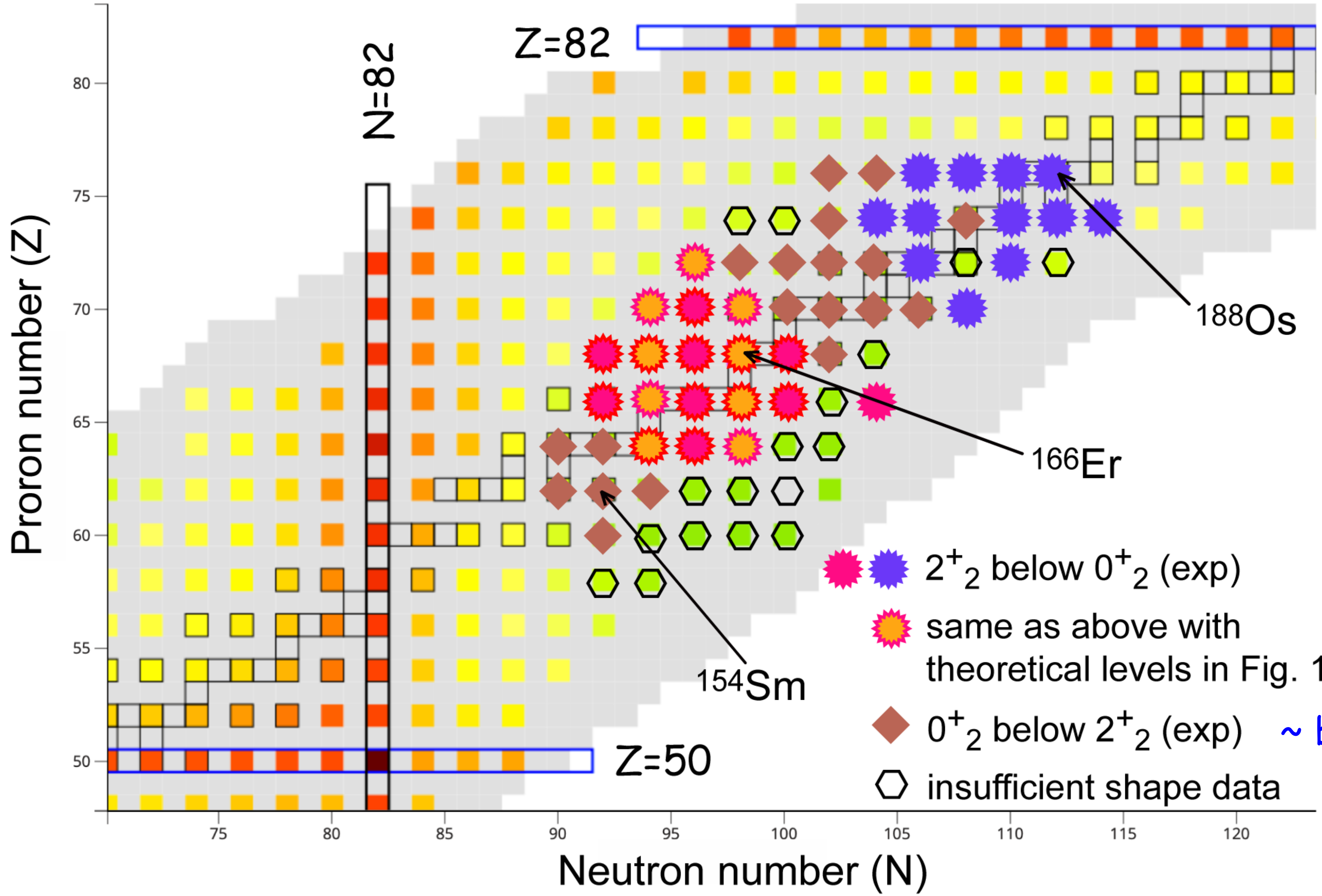

prominent triaxiality

~ basic triaxiality at most

Outline

1. Quantum many-body derivation of "rotational energy"

   conceptual but practical also

2. Triaxiality and rotational states

3. Vibrational excitations and triaxiality

Rotational states of a microscopic object are relevant to Quantum Computing

→ Proper description/understanding needed

Vibrational excitations

They can be searched by solving the eigenvalue problem with an increased number of basis vectors, yielding more eigenstates.

Usual T plot for the probability.

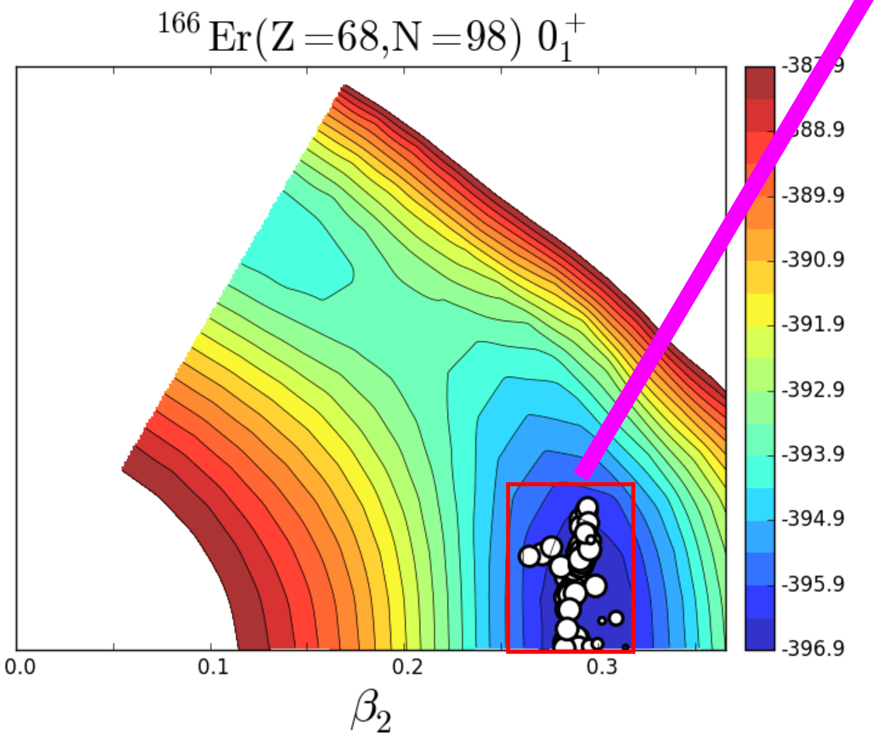

An advanced T-plot for mixing amplitudes

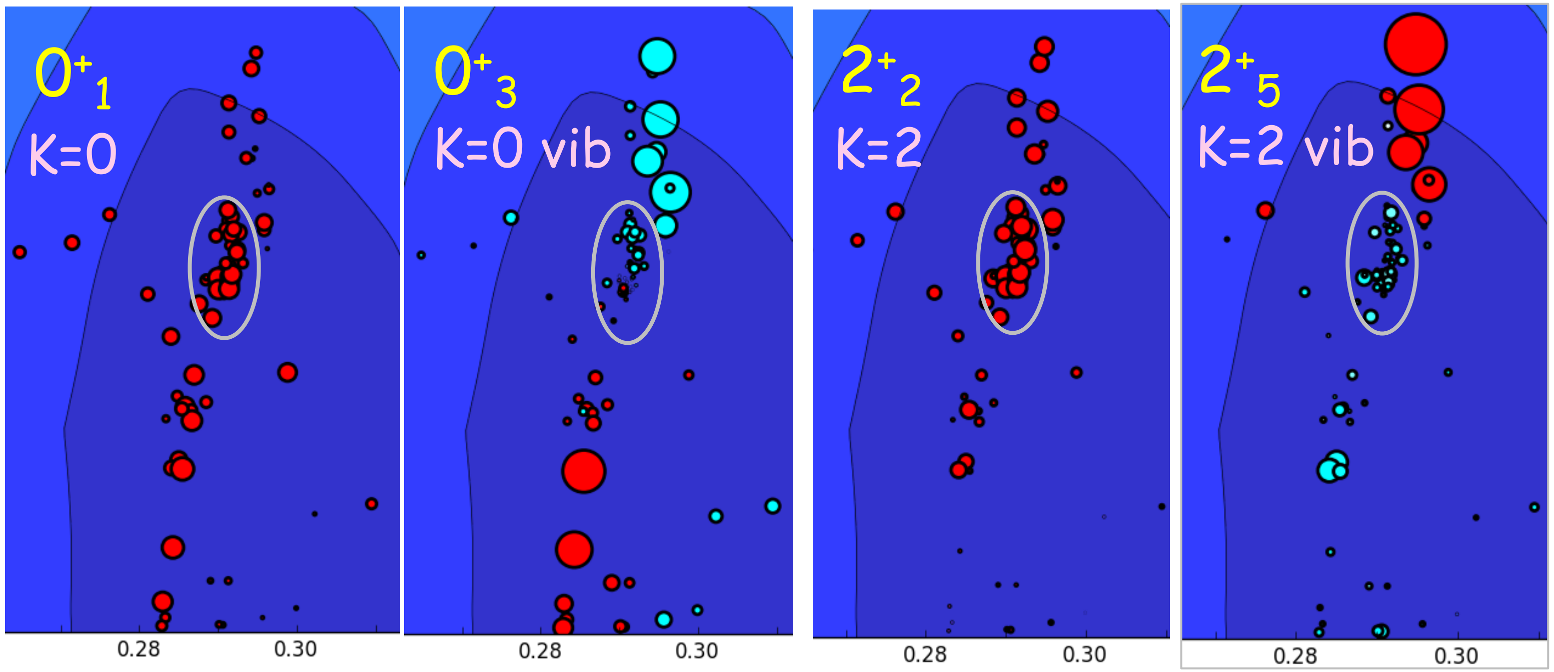

red (blue) circles : amplitudes are positive (negative)

amplitudes are defined to be positive for 0^+_1 or 2^+_2 state

schematic illustration

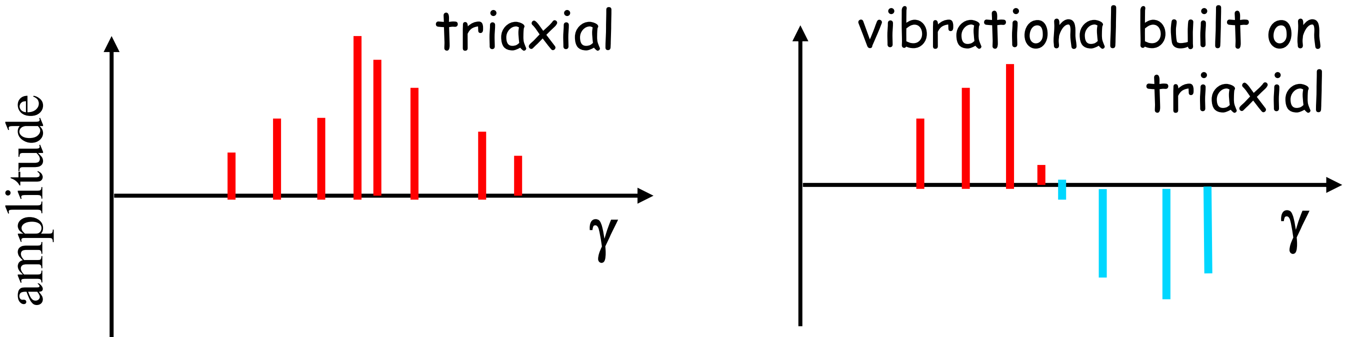

Level energies of ^{166}Er including vibrational states

more deformed band (less triaxial, not β vibrational)
πg7/2 -> d3/2

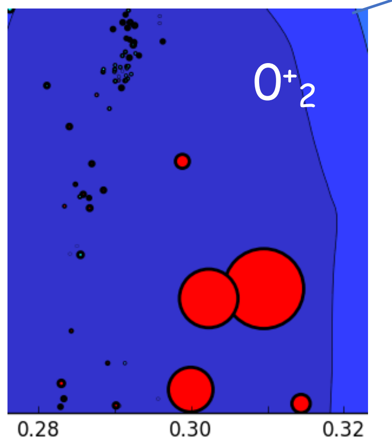

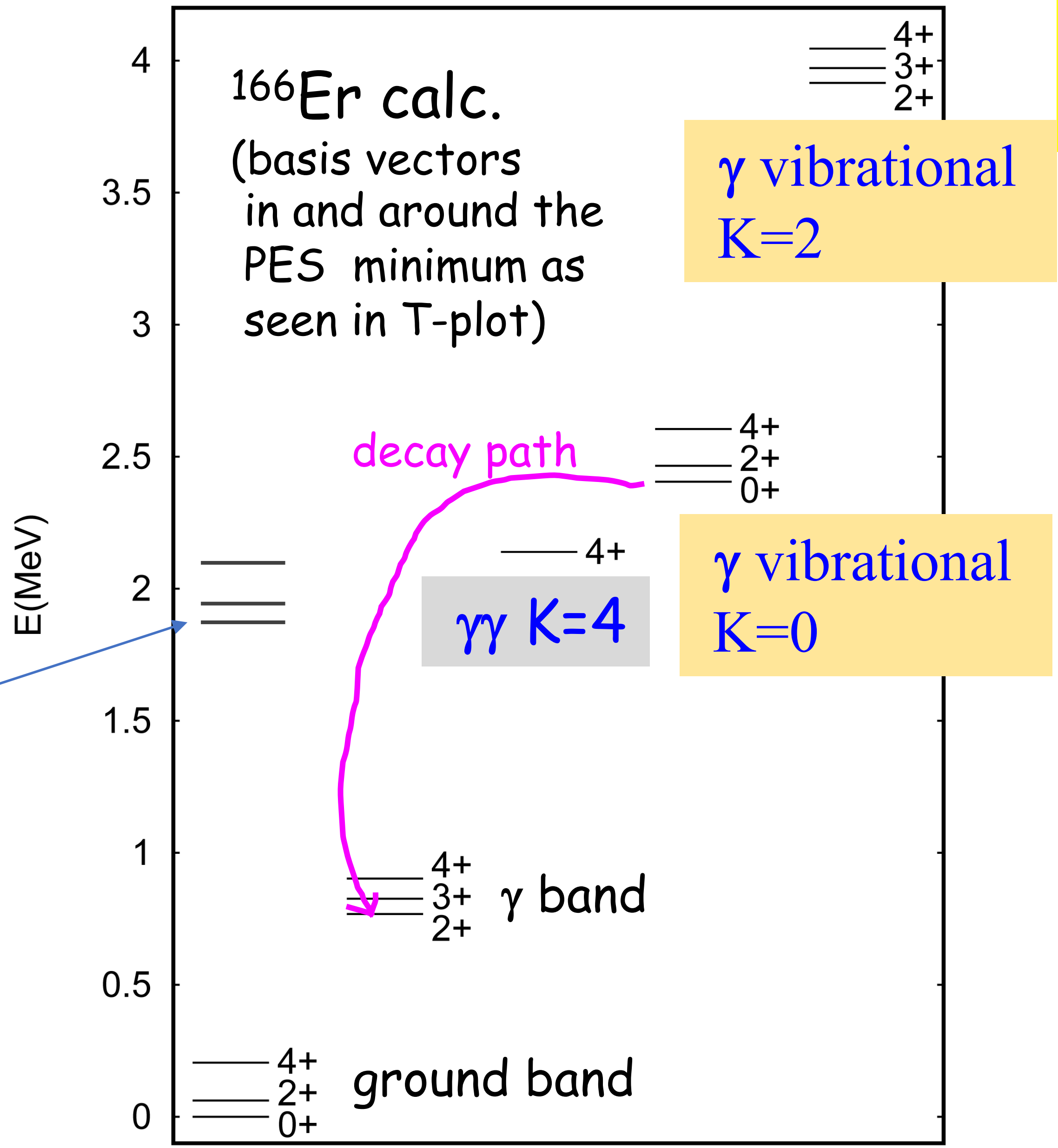

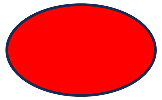

xy plane cross section of triaxial states

xy plane cross section of γ vibrational states built on triaxial states

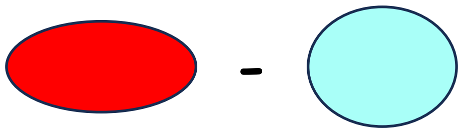

→ both K=0 and K=2 arise

K=2 ex. energy is higher by the same reason as that for the $2^+\gamma$ band

Summary

1. Rotational excitation energy proportional to $J(J+1) - K^2$ is derived in quantum many-body framework, without resorting to the quantization of the free rotation of classical rigid body.
2. Triaxial deformation occurs in virtually all deformed nuclei, because the symmetry restoration gives more binding energy than axially symmetric shapes. → "**basic triaxiality**"
3. Stronger triaxiality occurs, already for unprojected states, due to tensor (monopole) and/or central (hexadecupole) forces in some nuclei, at least in 13 rare-earth nuclei, such as ^{166}Er, ^{164}Dy, ^{158}Gd. → "**prominent triaxiality**"
4. **Vibrational excitations** from triaxial shapes are identified at Ex=2.5-4 MeV with K=0 and K=2. $\gamma\gamma$ K=4 and more deformed K=0 are seen, probably in agreement with experiment.
5. Nilsson and Davydov models are extended/assessed, but not discussed due to time.

Reference: **Prevailing Triaxial Shapes in Atomic Nuclei and a Quantum Theory of Rotation of Composite Objects**

arXiv:2303.11299v6 [nucl-th]

T. Otsuka,[1,2,3,4,*] Y. Tsunoda,[5,6] N. Shimizu,[6,5] Y. Utsuno,[7,5] T. Abe,[8,2] and H. Ueno[2]

Expecting a lot to come

E N D

Thank you for your attention

Appearance of (ground-state) rotational bands in nuclei

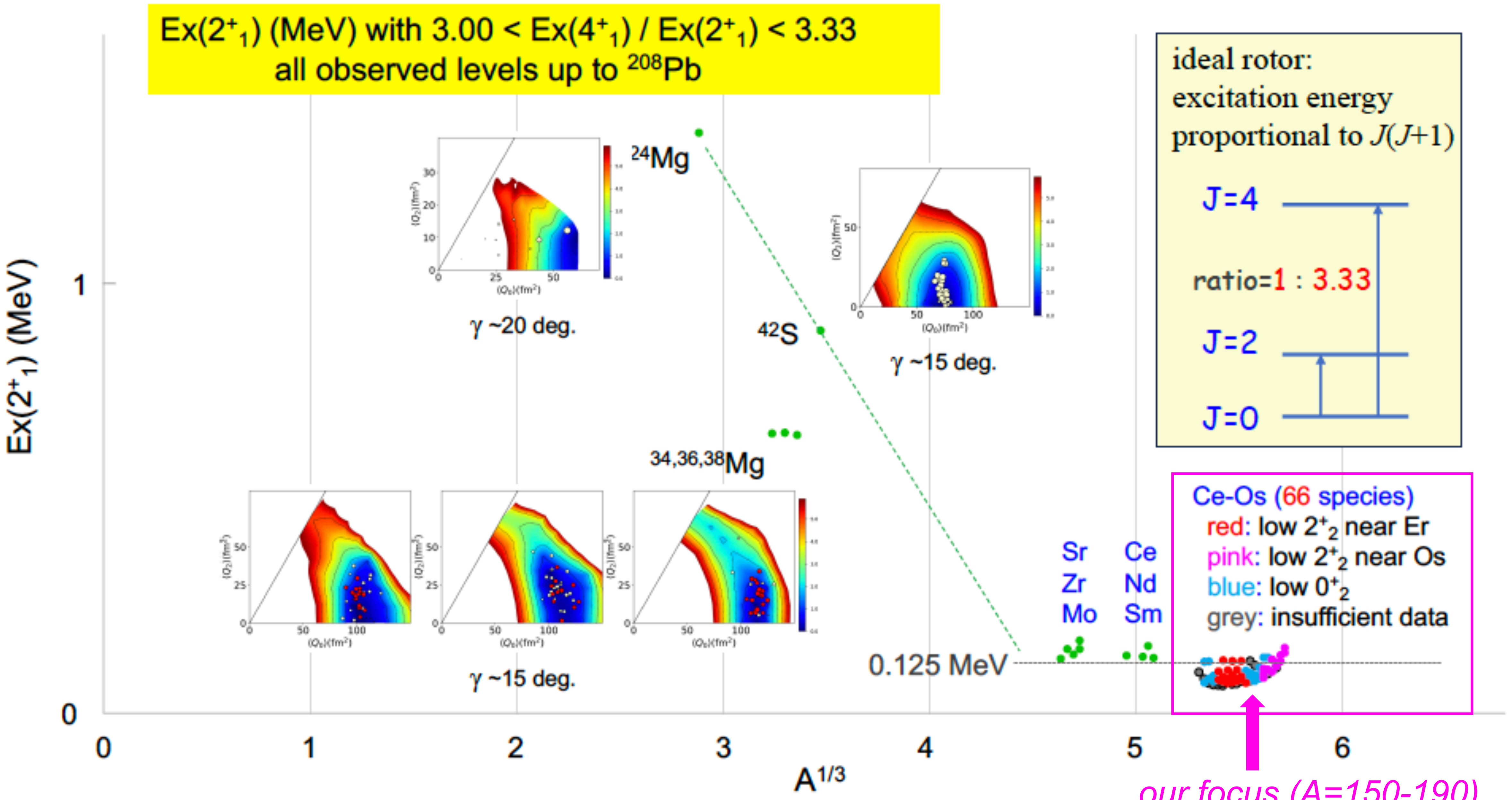

ideal rotor:
excitation energy
proportional to $J(J+1)$

J=4

ratio=1 : 3.33

J=2

J=0

our focus (A=150-190)

^{154}Sm : typical example of basic triaxiality only

no flat bottom in the unprojected PES

modest minimum in K / J projected PESs

Energy of unprojected state relative to γ=0 value as a function of γ

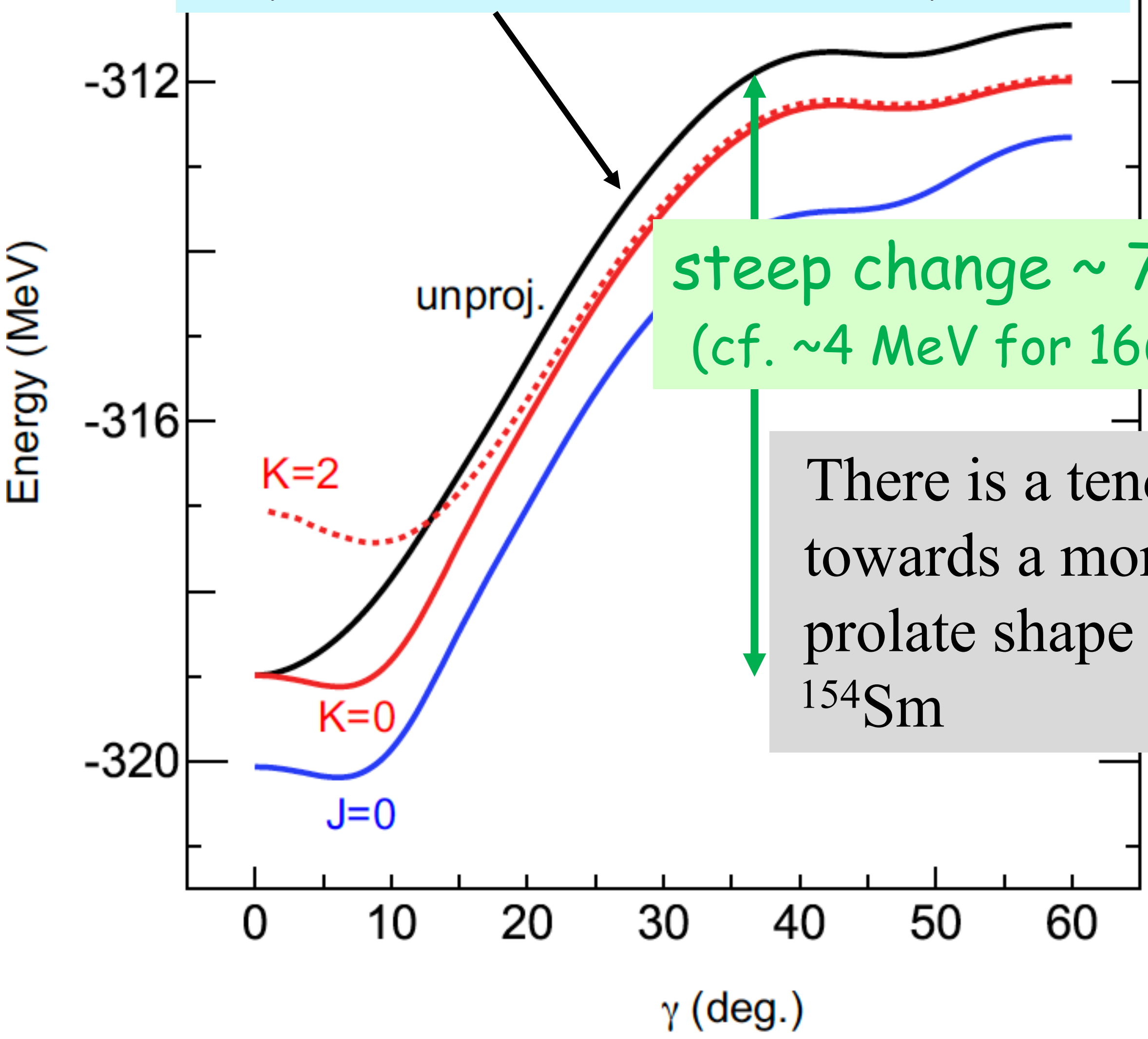

steep change ~ 7 MeV
(cf. ~4 MeV for 166Er)

There is a tendency towards a more prolate shape in ^{154}Sm

level energies

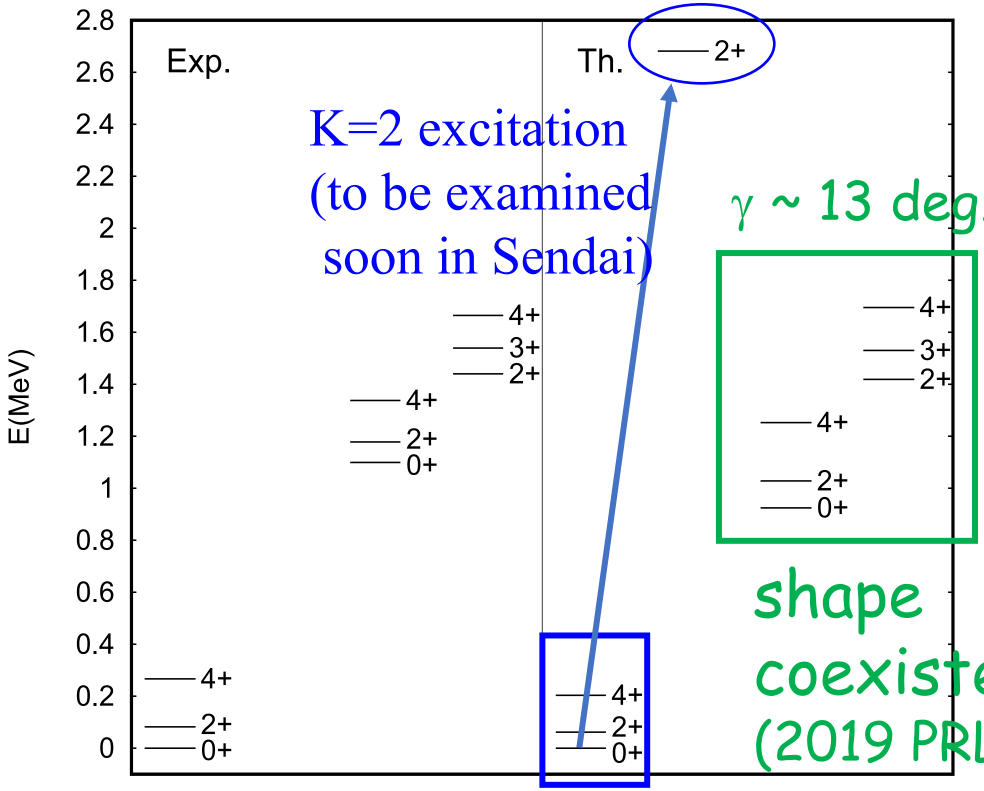

K=2 excitation
(to be examined soon in Sendai)

γ ~ 13 deg.

shape coexistence (2019 PRL)

γ ~ 4 deg.

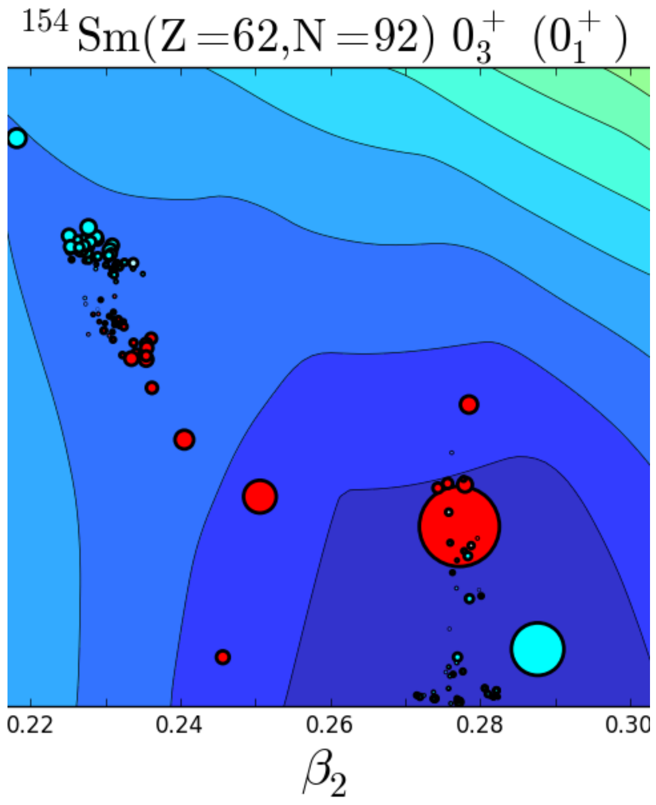

^{154}Sm(Z =62,N =92) 0_3^+ (0_1^+)
0.22
0.24
0.26
0.28
0.30
β_2

2. 82

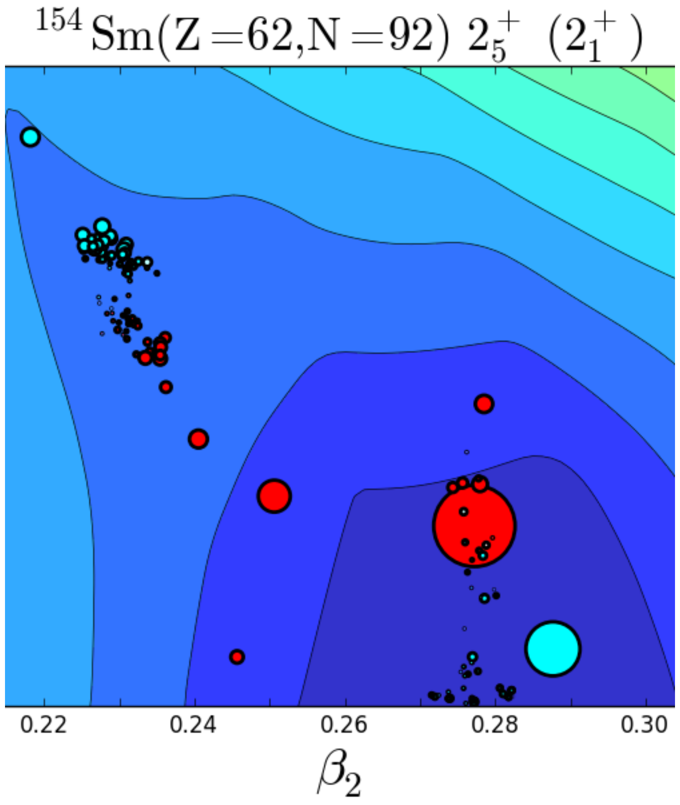

^{154}Sm(Z =62,N =92) 2_5^+ (2_1^+)
0.22
0.24
0.26
0.28
0.30
β_2

2. 88

Two major origins of triaxiality

1. Restoration of broken rotational symmetry in the intrinsic state

2. Specific components of *NN* interaction
   … effects seen in unprojected energy as flat bottom or basin
   before the symmetry restoration

Involvement of large-j orbitals are crucial for triaxiality

Hexadecupole central interaction does not work without them

Hexadecupole interaction favors more complicated shapes → triaxiality
Quadrupole interaction does not favor triaxiality, being neutral for unprojected PES

tensor monopole + central monopole push them down !

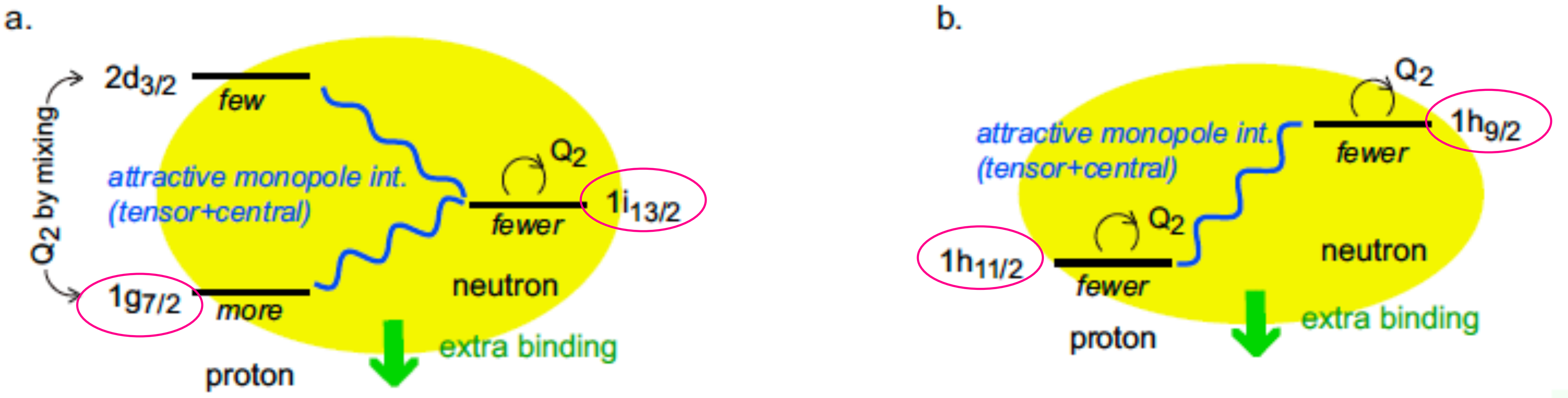

FIG. 12. Two basic modes giving more binding energies to states of triaxial shapes. The blue wavy line indicates proton-neutron monopole interaction (see eq. (68)) which is particularly strongly attractive due to coherent contribution from tensor and central interactions. The enhancement of the Q_2 (implicitly including Q_{-2}) quadrupole moment is indicated by arrows.

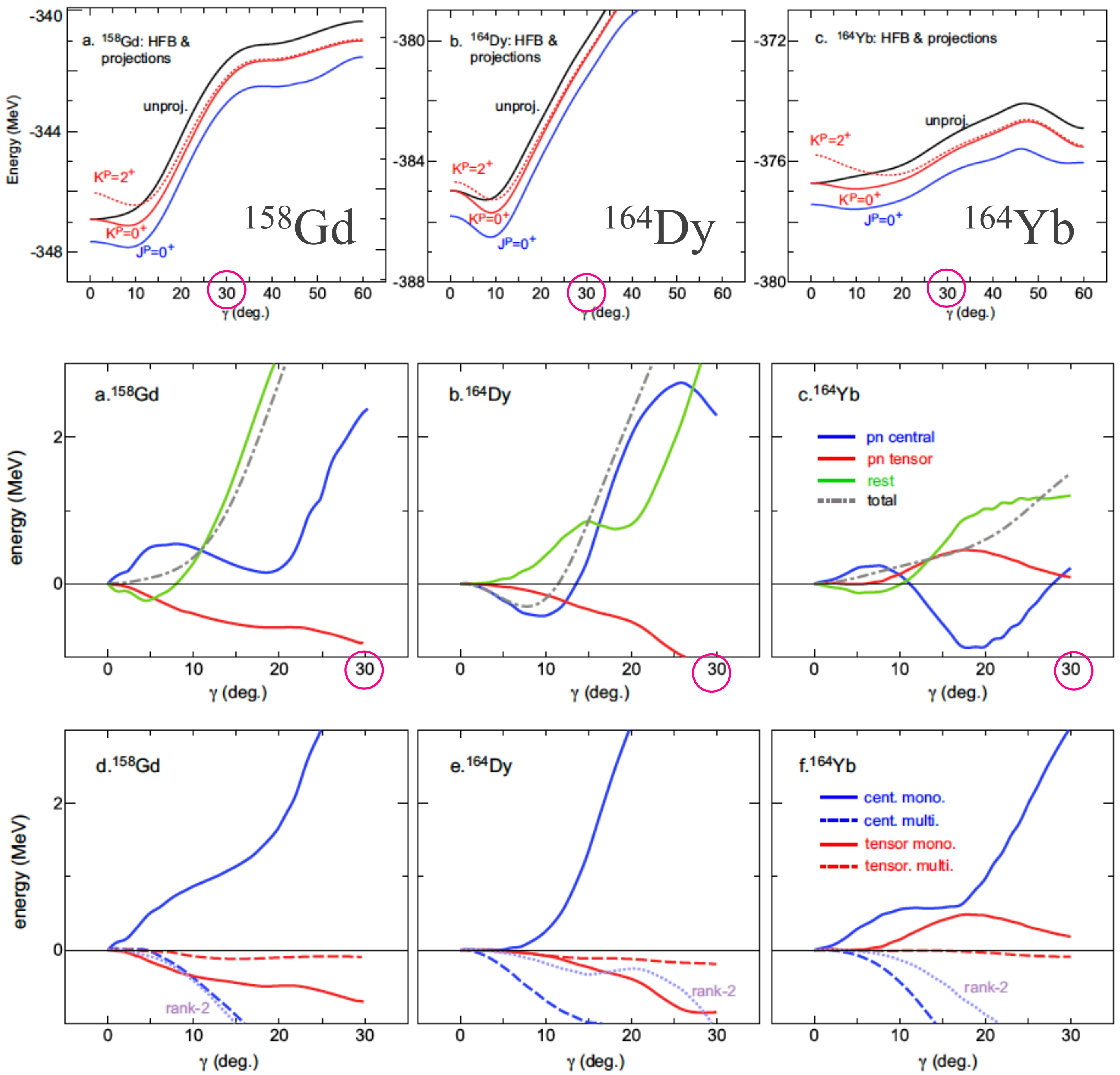

HFB PES decompositions

^{158}Gd (Z=64, N=94)

largely by tensor monopole,
the rest gives minor contribution,
γ = 5.9 deg.

^{164}Dy (Z=66, N=99)

mainly by hexadecupole int.,
also by tensor int.,
γ = 7.3 deg.,
most profound minimum

^{164}Yb (Z=70, N=94)

also by hexadecupole int.,
tensor neutral (flat),
γ = 8.7 deg.,
very flat

Evolution (stretching) of deformation parameter γ from ground to γ & $\gamma\gamma$ bands

K & J projections of the first (n=1) MCSM basis vectors

$n=1$ of $|\Psi\rangle = \sum_n f_n P^{J\pi} |\psi_n\rangle$

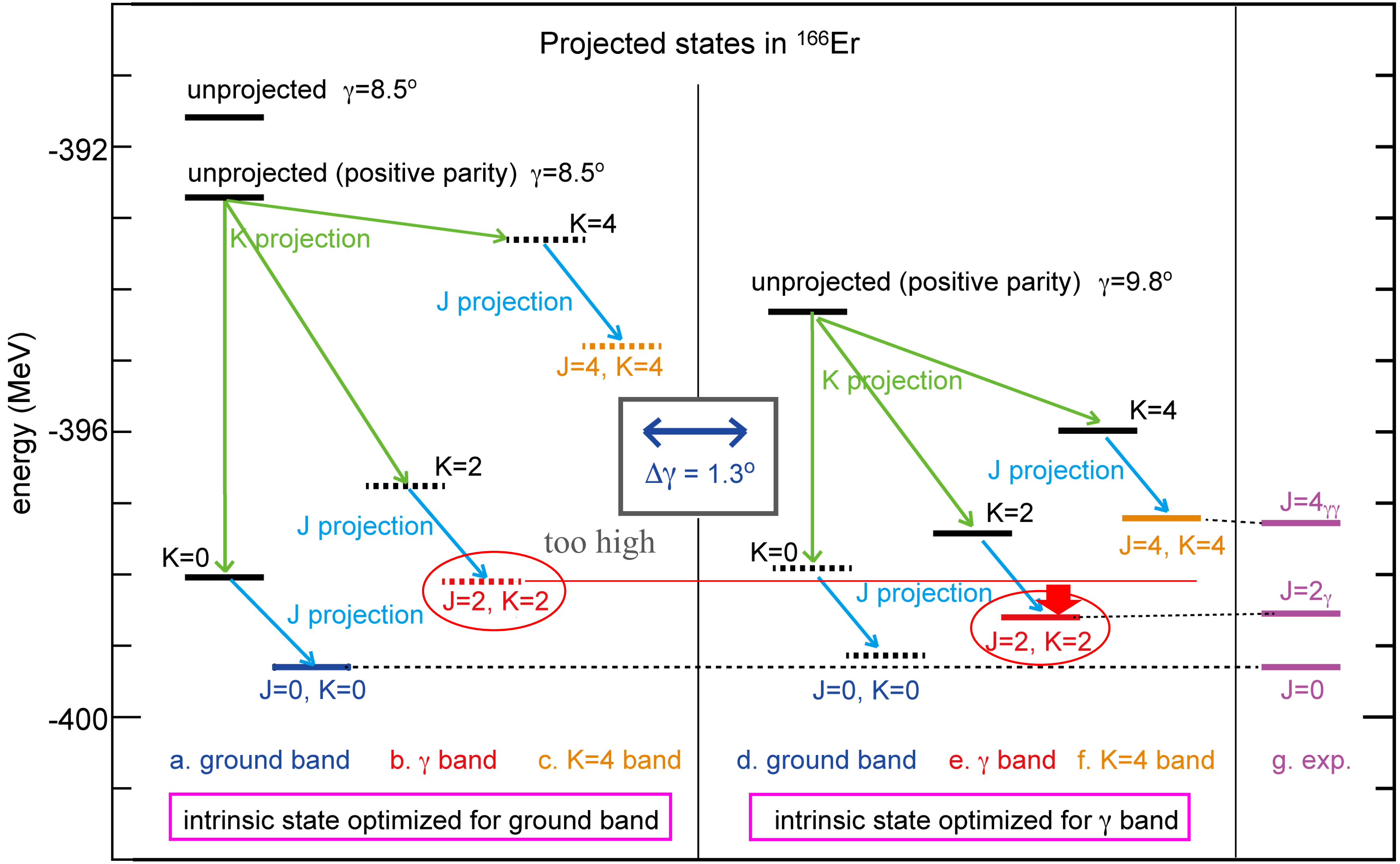

lowering of 2^+_γ level :
partly because of "opposite mechanism" weakened by a larger γ value (stretching in a quantal way)

next page

Broken rotational symmetry in the xy plane as represented by the ellipse.

This symmetry is restored by the projection onto a good K value

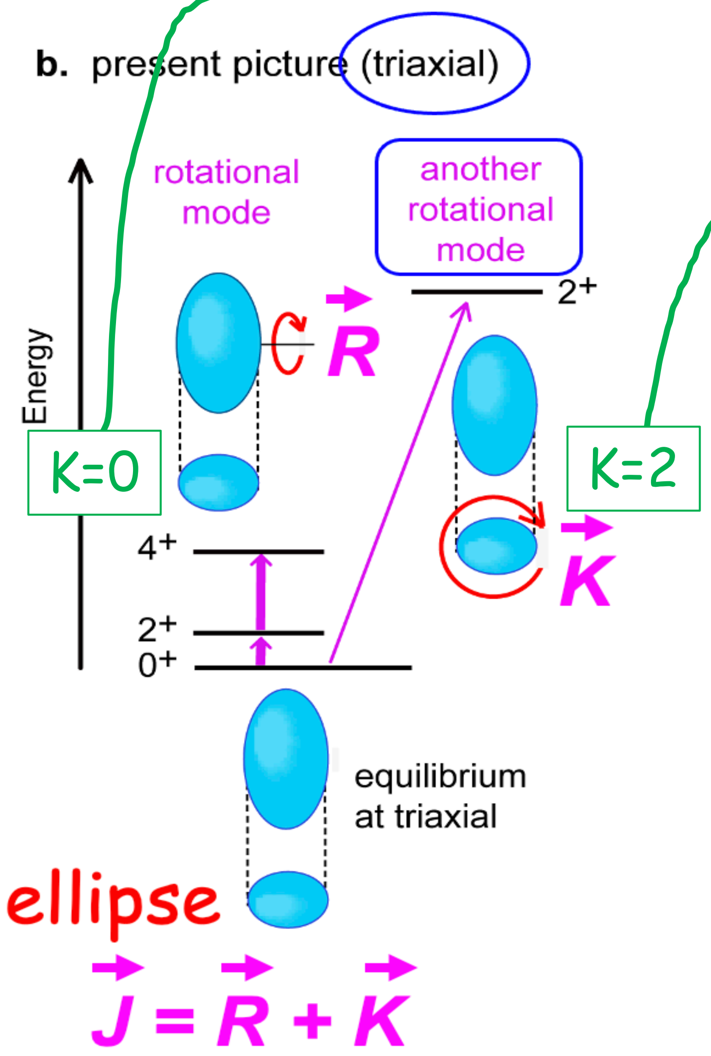

Euler angle γ	0		$\pi/4$		$\pi/2$		$3\pi/4$	

state (different representations of the 2-dim. rotational group)

(a) K = 0 $\Phi \propto$		+ … +		+ … +		+ … +		+ … +
(b) K = 2 $\Phi \propto$		+ … + i		+ … -		+ … - i		+ … +
(c) K = -2 $\Phi \propto$		+ … - i		+ … -		+ … + i		+ … +

Expectation value of H

non-zero triaxial deformation
→ more binding energy

(d) K = 0 (diagonal)

< K=0 |H| K=0 > $\propto$ < |H| > + … + < |H| > + … + < |H| >

+ … + < |H| > + … +

opposite

(e) K = 2 + K = -2 (diagonal)

< K=2&-2 |H| K=2&-2 > $\propto$ < |H| > + … + 0 ~~< |H| >~~ + … - < |H| >

+ … + 0 ~~< |H| >~~

less binding energy than K=0

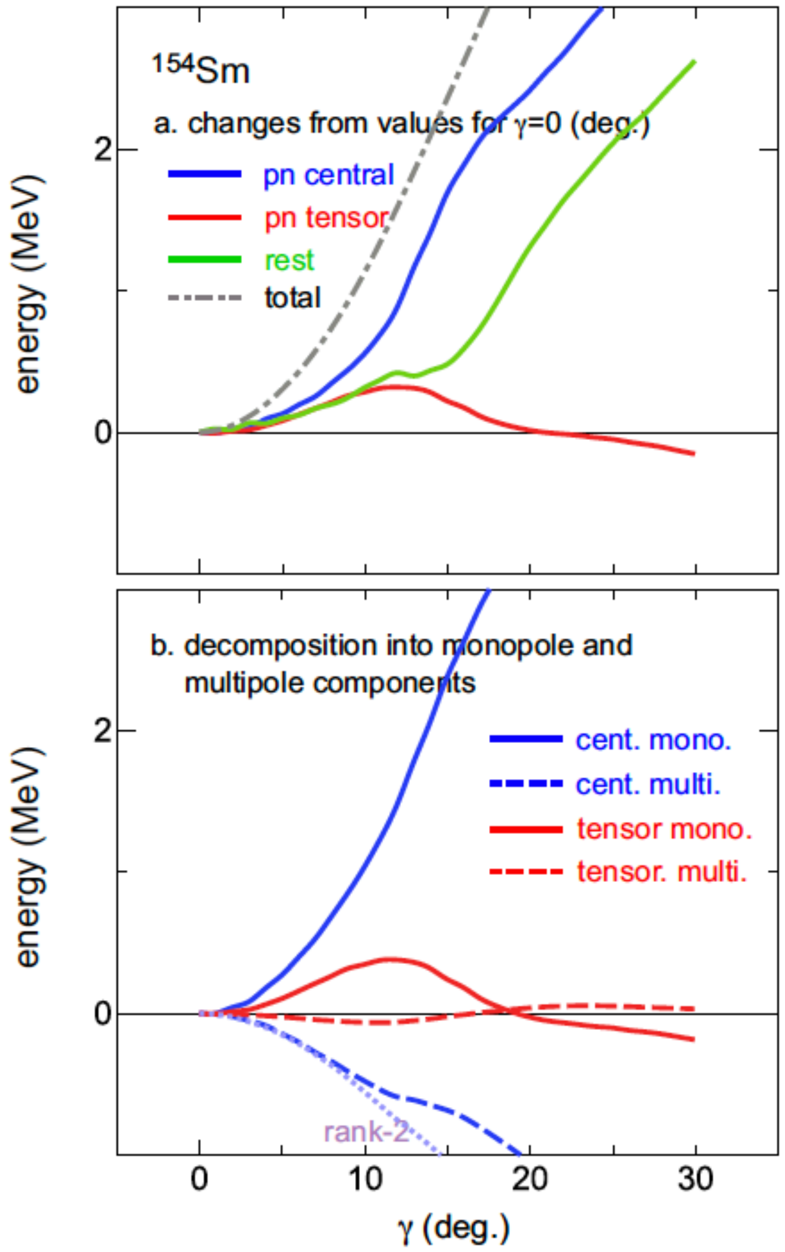

Decomposition into
pn central, pn tensor and rest components

… all repulsive up to γ ~20 deg

Further decomposition into monopole and multipole components → major players

No central high-rank multipole (hexadecupole) int.
&
Opposite tensor monopole int.

quadrupole int. dominates pn central multipole effects

A very different situation from the nuclei discussed so far

Example of basic triaxiality

^{154}Sm : basic triaxiality (gamma~3.7 deg.) in the ground band

prominent triaxiality (gamma~13 deg.) in the beta+gamma bands

shape coexistence

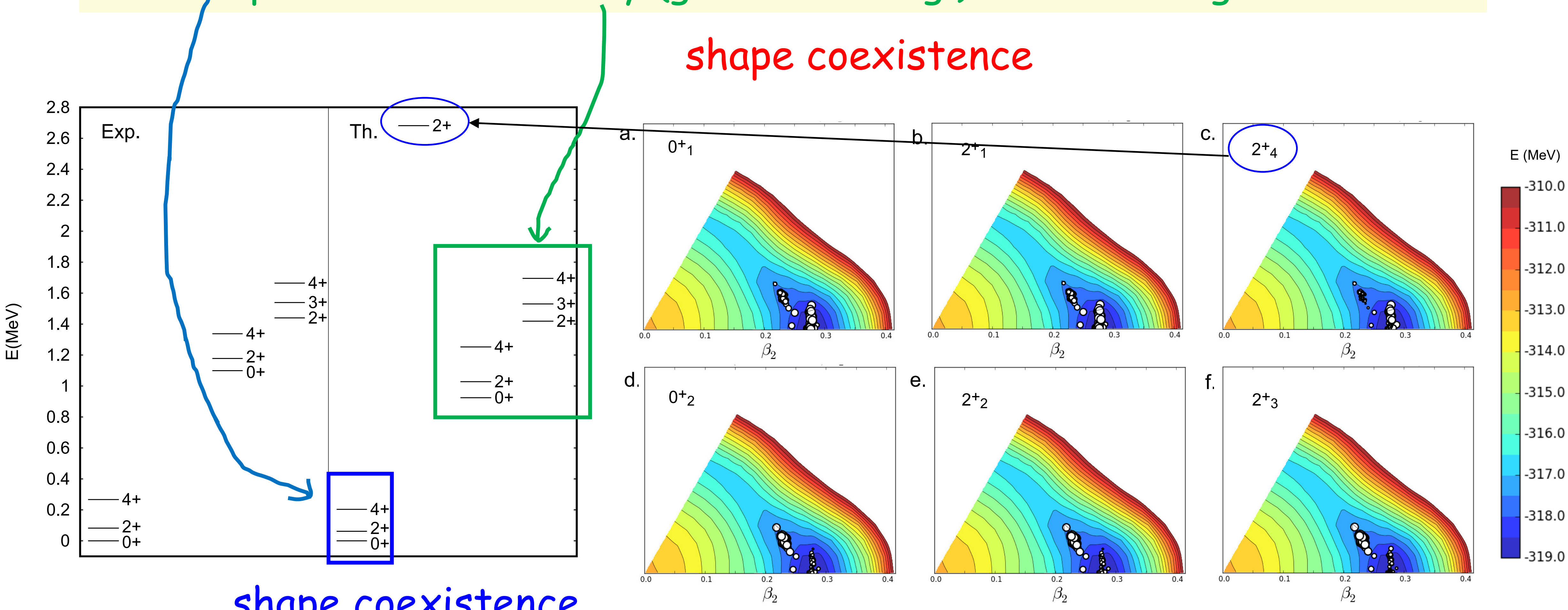

shape coexistence

Systematics of deformation parameter γ

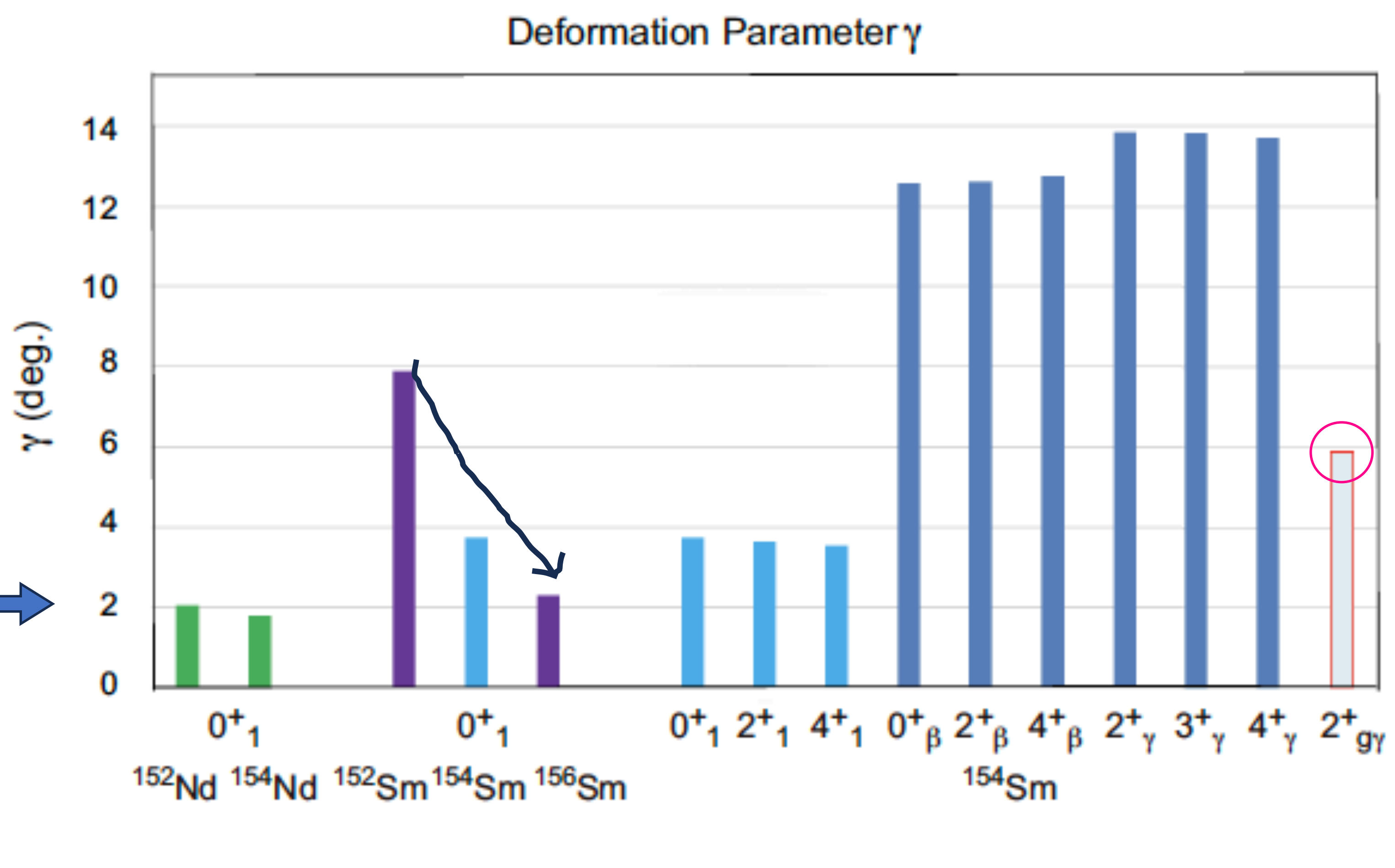

Is γ=2 degrees the minimum in this region of the Segre chart ?

Nilsson model

good feature of the Nilsson model is preserved by considering

odd particle x K=0^+ projected even-even core (incl. antisymmetrization)

This is an extended version of the Nilsson (+BCS) model
→ eNilsson (applicable also for prominent triaxial nuclei)

The quantum numbers of the Nilsson model can be used, even if the shape is prominent triaxial. → Merit of a faster and easier understanding !

Davydov model

The energies given by Davydov model may not be good enough because of the assumed rigid triaxiality. A stretching increases γ from g to γ and $\gamma\gamma$ bands.

The γ value from E2 transitions appears to be more precise.

It seems that the claimed triaxiality in strongly deformed nuclei could be appreciated more.

If γ = 9 degrees, 3γ =27 degrees, and

$$b(\mathrm{E2};\, 21 \to 0) = \frac{B(\mathrm{E2};\, 21 \to 0)}{\left(\frac{e^2 Q_0^2}{16\pi}\right)} = \frac{1}{2}\left[1 + \frac{3 - 2\sin^2(3\gamma)}{\sqrt{9 - 8\sin^2(3\gamma)}}\right], \quad (2.6)$$

→ $\frac{1}{2}$ [1 + 0.9510] = 0.9755

the ratio is 1 : 0.0251

$$b(\mathrm{E2};\, 22 \to 0) = \frac{1}{2}\left[1 - \frac{3 - 2\sin^2(3\gamma)}{\sqrt{9 - 8\sin^2(3\gamma)}}\right], \quad (2.7)$$

→ $\frac{1}{2}$ [1 - 0.9510] = 0.0245

experimentally this ratio is 1 : 0.024(1)

from Davydov & Filippov, Nucl. Phys. 8 (1958)

Davydov et al. addressed

Comparison of the predictions of the theory with the experimental data presently known to us thus confirms the assumption that some even nuclei do not possess axial symmetry.

Remark on double γ-phonon (γγ) state

$$n = 1 \text{ of } |\Psi\rangle = \sum_n f_n P^{J\pi} |\psi_n\rangle$$

K & J Projections of the first (n=1) basis vectors of MCSM (QVSM) for g and γ bands

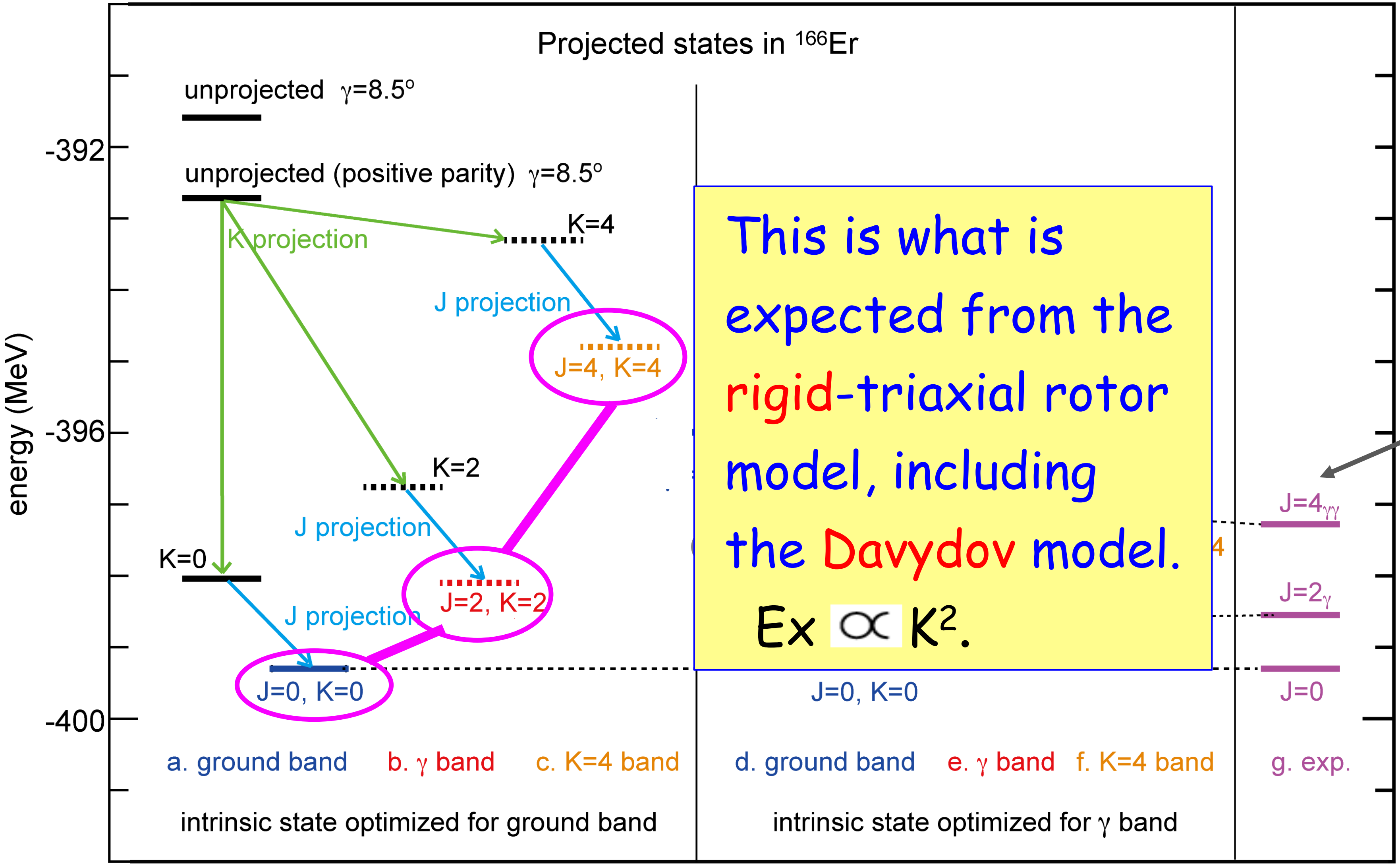

This is what is expected from the rigid-triaxial rotor model, including the Davydov model.

Ex ∝ K^2.

double γ-phonon (γγ) state (long-term mystery)

partly because of opposite mechanism weakened by larger γ value (stretching in a quantal way)

Remark on double γ-phonon (γγ) state (continued)

$$n = 1 \text{ of } |\Psi\rangle = \sum_n f_n P^{J\pi} |\psi_n\rangle$$

K & J Projections of the first (n=1) basis vectors of MCSM (QVSM) for g and γ bands

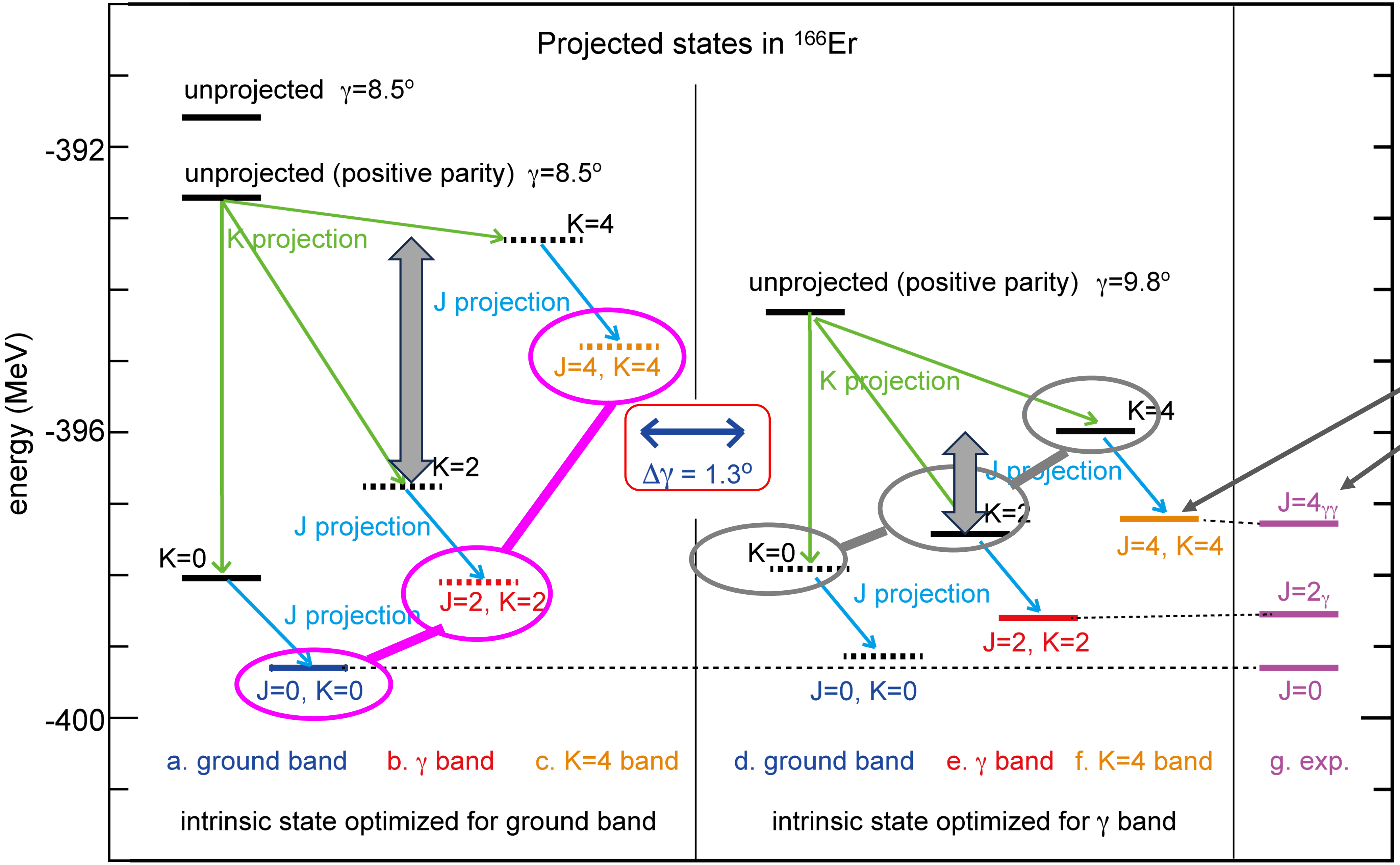

so-called double γ-phonon (γγ) state (long-term mystery) naturally appears as K=4 member

partly because of the stretching with a larger γ value in a quantal way

Summary

1. Rotational excitation energy proportional to $J(J+1) - K^2$ is derived in quantum many-body framework, without resorting to the quantization of the free rotation of classical rigid body.

2. Triaxial deformation occurs in virtually all deformed nuclei, because it gives more binding energy than axially symmetric shapes. → "**basic triaxiality**" It is not a fluctuation.
The ground band of ^{154}Sm is an example, while side bands show shape coexistence with γ.

3. Stronger triaxiality occurs due to tensor (monopole) and/or central (hexadecupole) forces in some nuclei, at least in 13 rare-earth nuclei, such as ^{166}Er, ^{164}Dy, ^{158}Gd.
→ "**prominent triaxiality**"

4. Nilsson model may be extended even to nuclei with triaxial shapes. (→ eNilsson model)

5. The prevailing triaxiality in strongly deformed nuclei proposed by Davydov may receive more appreciation, putting aside his model's rather poor predictive power for energies.

Reference: **Prevailing Triaxial Shapes in Atomic Nuclei and a Quantum Theory of Rotation of Composite Objects** arXiv:2303.11299v6 [nucl-th]

T. Otsuka,[1,2,3,4,*] Y. Tsunoda,[5,6] N. Shimizu,[6,5] Y. Utsuno,[7,5] T. Abe,[8,2] and H. Ueno[2]

Experimental test of triaxiality

Direct measurement of the shape is most desirable

Relativistic Heavy-Ion Collision

can also cover down to basic triaxiality.

Multiple Coulomb excitation (initiated by Doug Cline)

already (1990's) provided with consistent nice data with
not-so-natural interpretation *(preconceptions cloud your eyes)*

also for ^{166}Er by Fahlander et al. (1992), for ^{164}Dyand ^{158}Gd, by Werner, et al (2005).

renewed possibilities with *AGATA* and GRETA ($\Delta\gamma$ = 1 deg. will be great)

Other plausible possibilities … even up to EIC

various (e,e') like GDR or M1 excitations

and more

Types of ellipsoidal shapes of nuclei and comparison to molecules

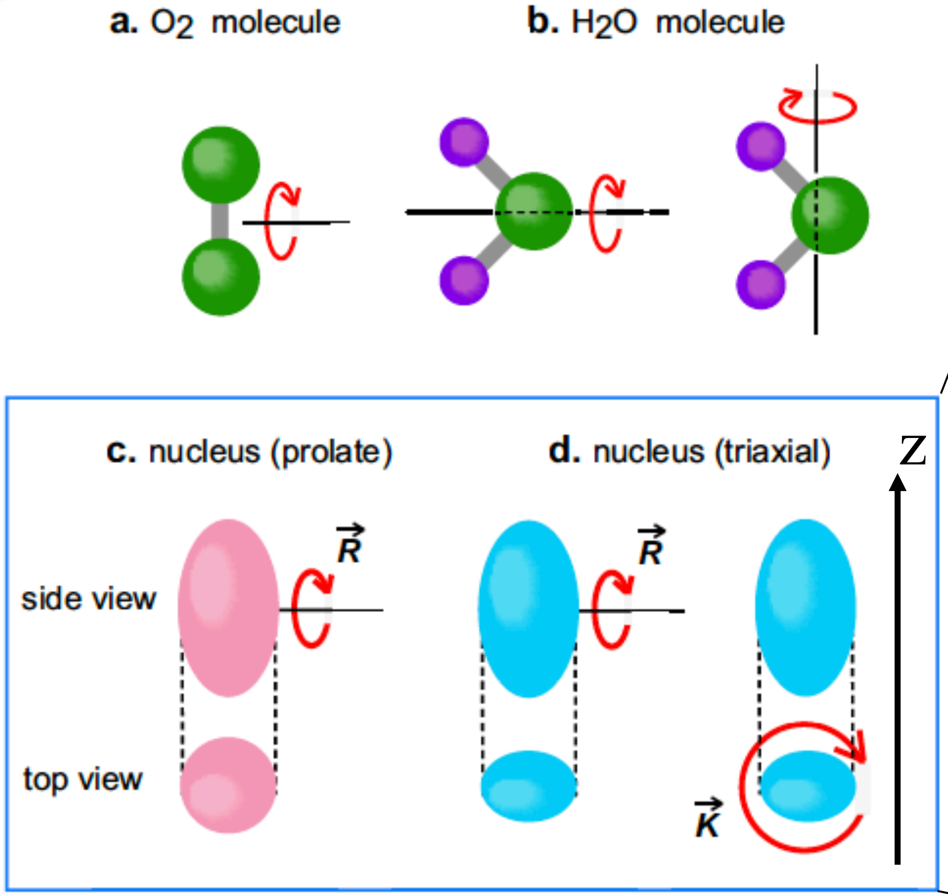

quadrupole moments of the intrinsic state (nuclear state in the body-fixed frame)

$$Q_0 = \langle 2z^2 - x^2 - y^2 \rangle$$

$$Q_2 = \sqrt{3/2}\,\langle x^2 - y^2 \rangle$$

deformation parameters

$$\beta_2^2 \propto (Q_0^2 + 2\,Q_2^2)$$

$$\tan\gamma = \sqrt{2}\,\frac{Q_2}{Q_0}$$

prolate shape	$\gamma=0°$	$Q_2 = 0$
triaxial shape	$\gamma \neq 0°$	$Q_2 \neq 0$
(oblate shape	$\gamma=60°$)	

Deformed (=non-spherical) objects rotate in classical and quantum senses.

PRL 97, 162502 (2006) PHYSICAL REVIEW LETTERS week ending 20 OCTOBER 2006

Global Calculations of Ground-State Axial Shape Asymmetry of Nuclei

Peter Möller,[1,*] Ragnar Bengtsson,[2] B. Gillis Carlsson,[2] Peter Olivius,[2] and Takatoshi Ichikawa[3]

Conventional view

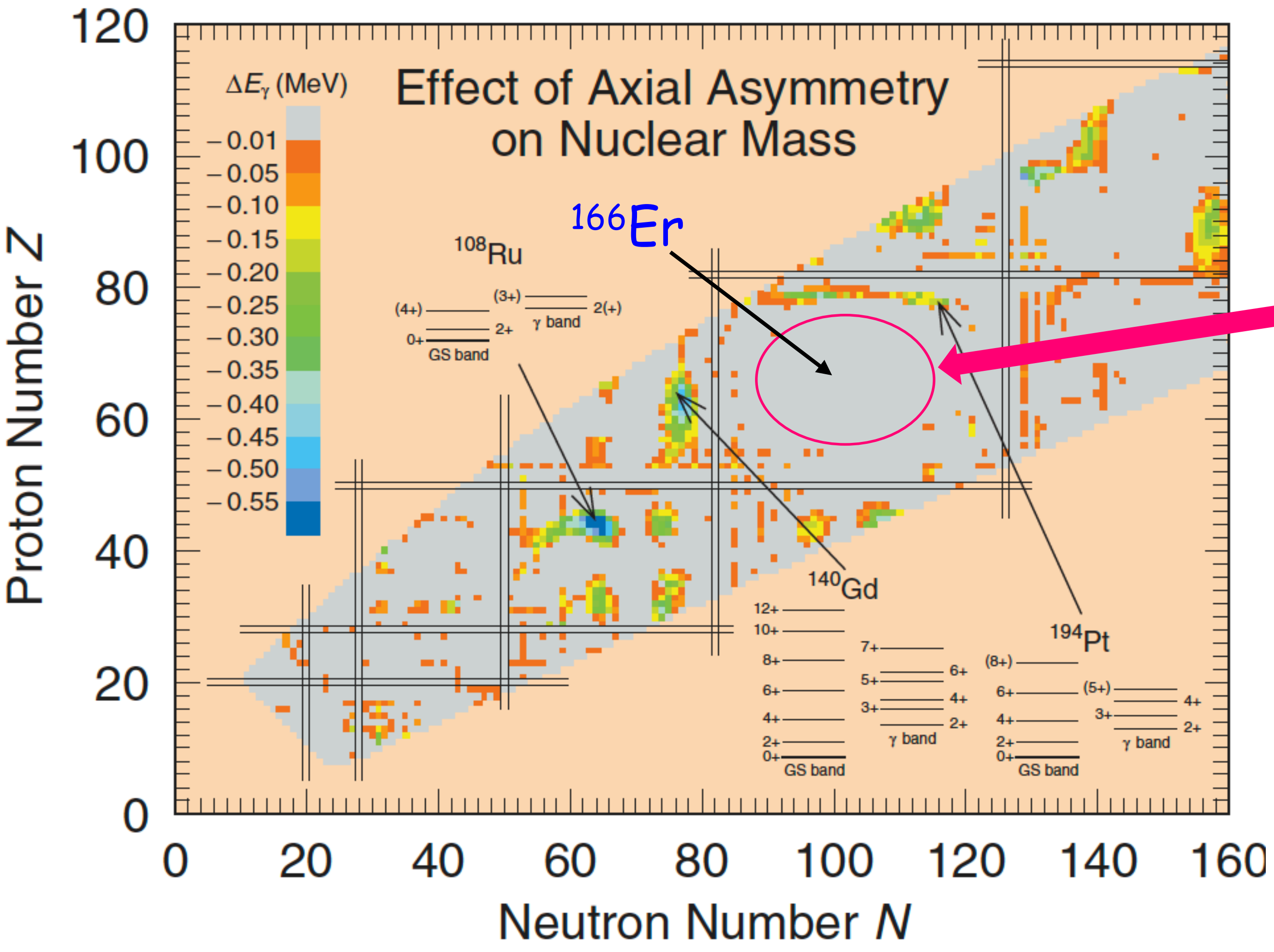

Axial symmetry supposed to dominate
the region of
current interest
a la Aage Bohr

Questions were raised from some viewpoints, but it remained unsettled.

Eur. Phys. J. A (2019) 55: 15
DOI 10.1140/epja/i2019-12665-x

THE EUROPEAN PHYSICAL JOURNAL A

Review

"Stiff" deformed nuclei, configuration dependent pairing and the β and γ degrees of freedom

J.F. Sharpey-Schafer[1,a], R.A. Bark[2], S.P. Bvumbi[3], T.R.S. Dinoko[4], and S.N.T. Majola[5,b]

Sharpey-Schafer *et al.* (2019) on γ-phonon

Data from Multiple CoulEx experiments showed finite γ values, but no explicit strong claim of triaxiality was made.

Cline et al (1986,1990), Fahlander et al (1992), Werner et al (2005), …

INSTITUTE OF PHYSICS PUBLISHING JOURNAL OF PHYSICS G: NUCLEAR AND PARTICLE PHYSICS

J. Phys. G: Nucl. Part. Phys. **27** (2001) R1–R22 www.iop.org/Journals/jg PII: S0954-3899(01)18337-4

TOPICAL REVIEW

Characterization of the β vibration and 0_2^+ states in deformed nuclei

P E Garrett

on β-phonon or β vibration

P. Boutachkov, A. Aprahamian, Y. Sun, J.A. Sheikh & S. Frauendorf

The European Physical Journal A - Hadrons and Nuclei **15**, 455–458 (2002)

empirical approach

Furthermore, there have been microscopic approaches also, where the description of excited bands are still a challenge.

Gogny -> 5DCH
(Bohr-Hamiltonian)

Delaroche et al.,
PR C 81, 014303 (2010)

Correlations between theoretical & experimental values (scale: logarithmic)

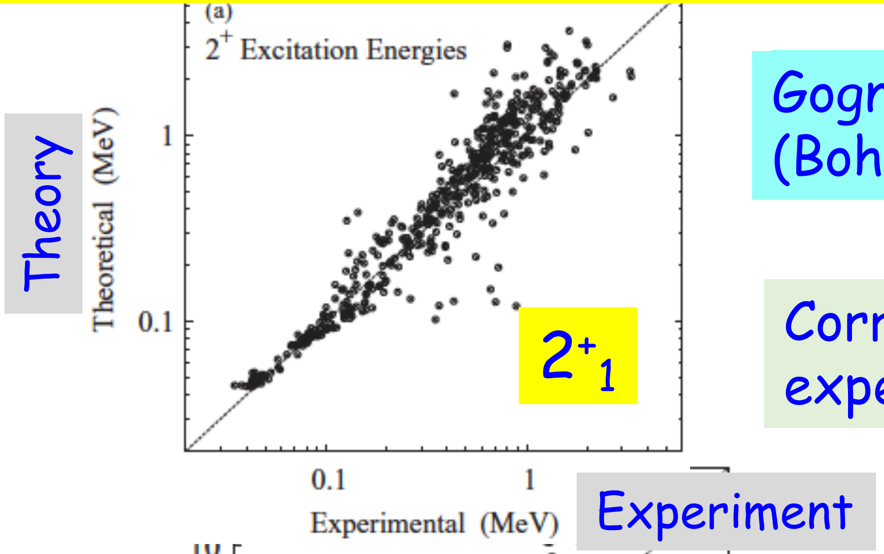

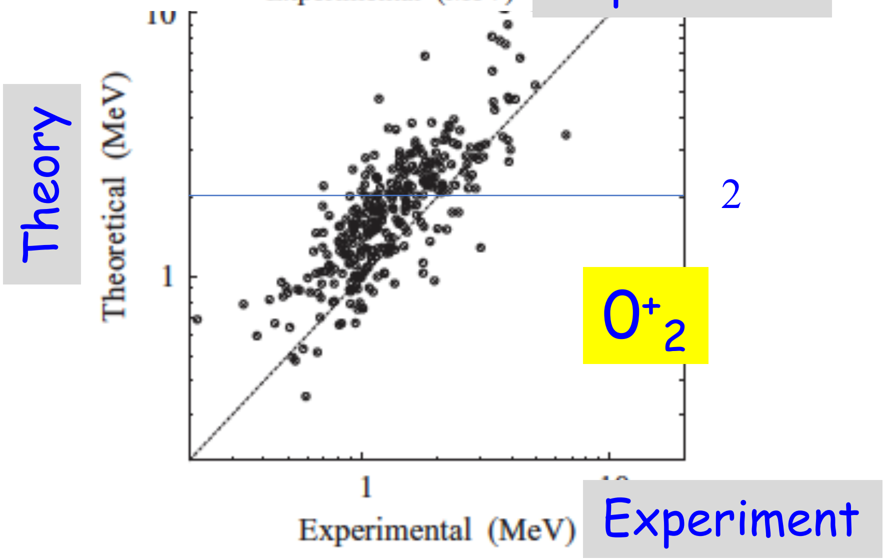

FIG. 20. Excitation energy of the 0_2^+ state compared with experiment [24].

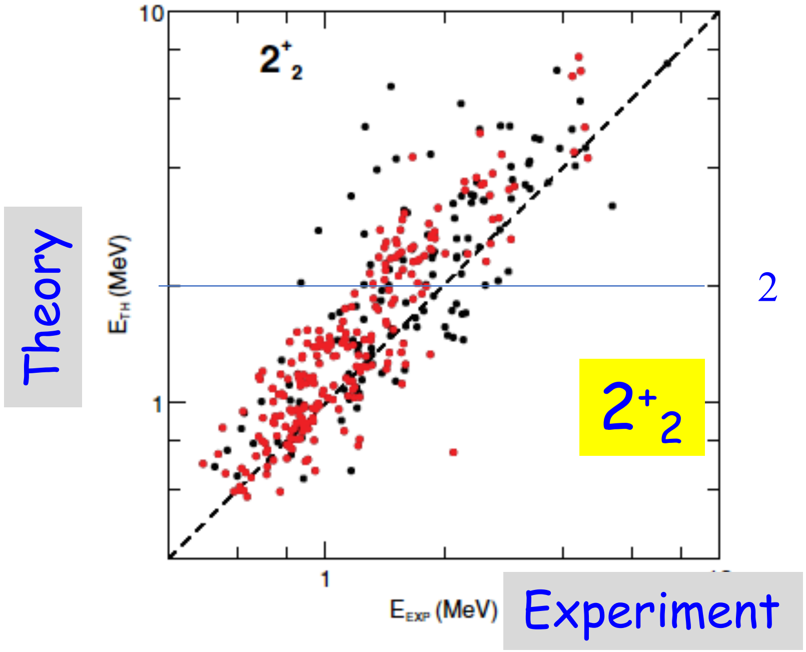

FIG. 19. (Color online) Excitation energy of the second $J = 2$ excitation, comparing 352 nuclei. Experimental data are from Ref. [24]. The 2_γ^+ levels are marked with red color.

Basic formulation of Monte Carlo Shell Model

N_B : number of basis vectors

eigenstate

$$\left|\Psi(D)\right\rangle = \sum_{n=1}^{N_B} c_i P^{J,\Pi} \left|\phi(D^{(n)})\right\rangle$$

amplitude

Projection op.

N_p : number of (active) particles

N_{sp} : number of single-particle states

$$\left|\phi(D^{(n)})\right\rangle = \prod_{\alpha=1}^{N_p} \underbrace{\left(\sum_{i=1}^{N_{sp}} a_i^\dagger D_{i\alpha}^{(n)}\right)}_{\text{Superposition of original single-particle state}} \left|-\right\rangle$$

n-th basis vector (Slater determinant)

Superposition of original single-particle state

Bogoliubov state in the QVSM (advanced version)

$$E(D) = \left\langle\Psi(D)\middle|H\middle|\Psi(D)\right\rangle$$

Minimize *E(D)* with respect to *D* utilizing Quantum MC and variational methods

Step 1 : Shift randomly matrix matrix D. (The initial guess can be taken from Hartree-Fock.)
Select the one producing the lowest *E(D)* (rate < 0.1 %)

Step 2 : Polish *D* by means of the conjugate gradient (CG) method variationally.

Identification of nuclear shape by T-plot of MCSM

- Location of circle: shape
  quadrupole deformation of unprojected MCSM basis vector

- Area of circle: importance
  overlap probability between each projected basis vector and the eigen wave function

- Potential energy surface (PES) is calculated by Constrained HF for the same interaction

T-plot of 0^+ states of ^{78}Ni (Z=28, N=50)

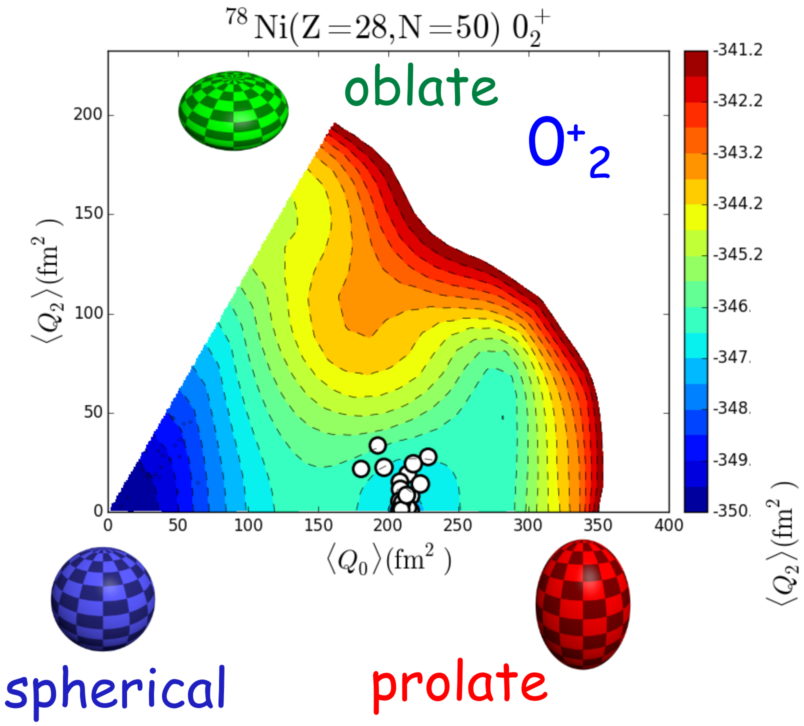

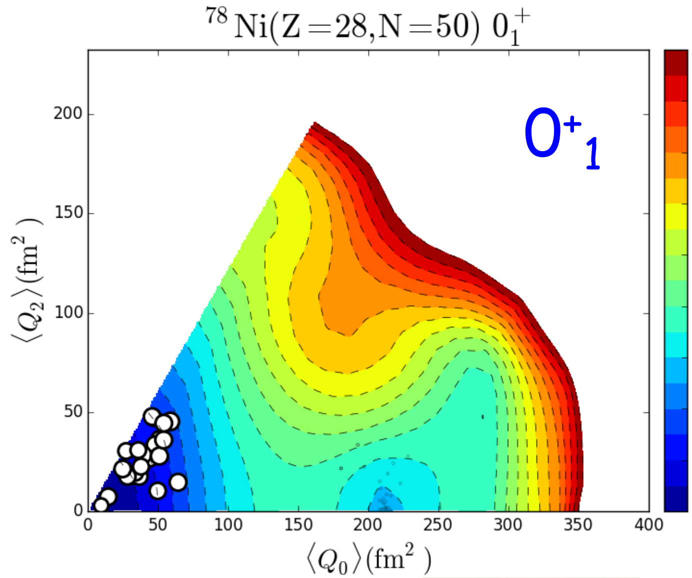

angular-momentum, parity projection

Slater determinant or Bogoliubov states (BCS with deformation)

$$\boxed{|\Psi\rangle} = \sum_n f_n \boxed{P^{J\pi}|\psi_n\rangle}$$

MCSM eigen wave function

MCSM basis vector

Y. Tsunoda, *et al.*
PRC 89, 031301 (R) (2014)

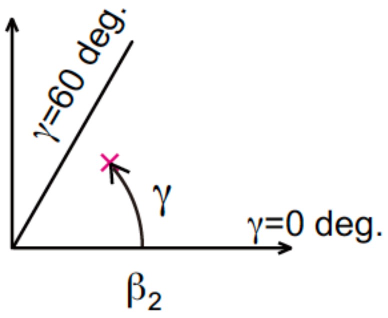

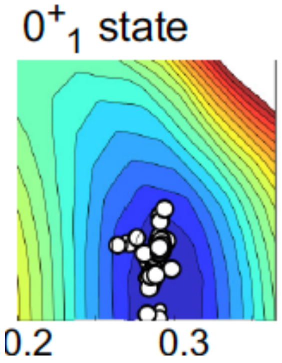

A remark about fluctuations or variances after orthogonalization (preliminary)

			β_2		γ (deg.)	
			mean value	standard deviation	mean value	standard deviation
^{166}Er	0^+_1	ground state	0.292	0.006	8.2	2.3
	2^+_2	γ band head	0.294	0.005	9.1	1.7
	4^+_3	$\gamma\,\gamma$ band head	0.294	0.005	9.5	1.5
^{154}Sm	0^+_1	ground state	0.275	0.011	3.7	2.9
	0^+_2	β band head	0.240	0.010	12.6	3.8
	2^+_4	gγ band head	0.278	0.009	5.9	2.6

valence nucleons are sparsely configured because of the shell structure

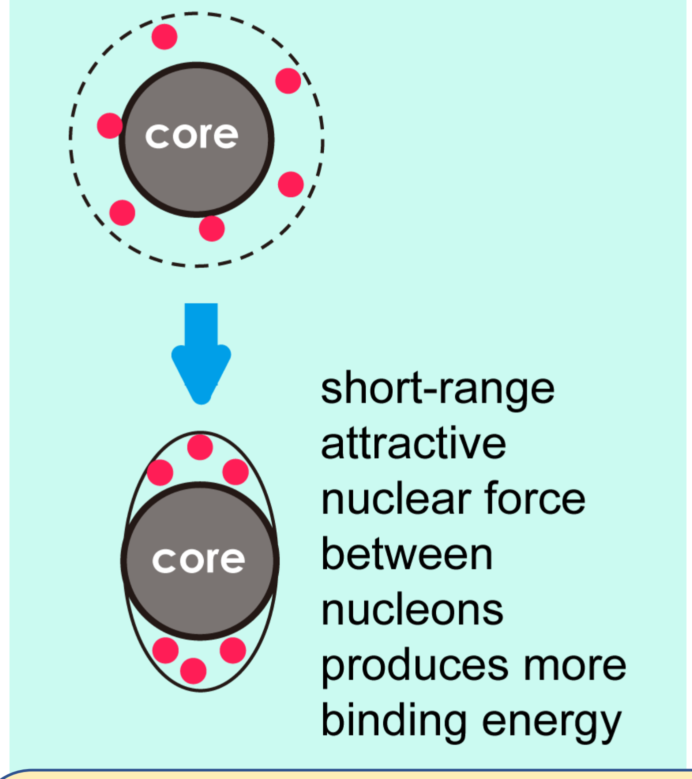

range of nuclear forces
<<
size of single-particle orbital
(the bigger the heavier)

b. Level energies of atomic nuclei with spherical and ellipsoidal shapes (examples)

c. All measured lowest 2^+ level energies (as of 2022)

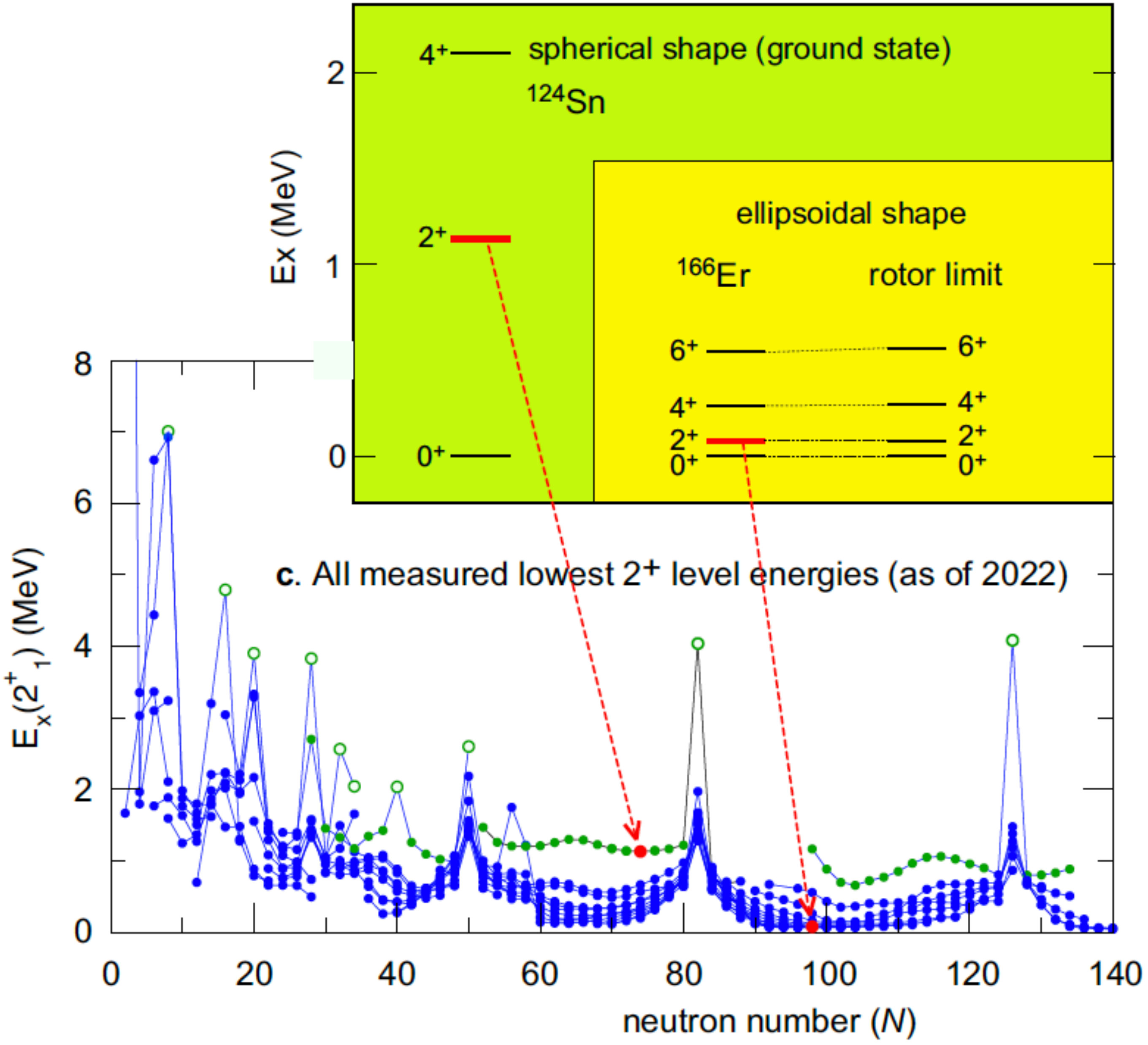

γ-decay of the Isovector Giant Dipole Resonance of ^{154}Sm: Smekal-Raman Scattering as a Novel Probe of Nuclear Ground-State Deformation

J. Kleemann,[1,*] U. Friman-Gayer,[2,3,†] J. Isaak,[1] O. Papst,[1] N. Pietralla,[1] K. Prifti,[1] V. Werner,[1] A. D. Ayangeakaa,[4,3] T. Beck,[1,‡] G. Colò,[5] M. L. Cortés,[1] S. W. Finch,[2,3] M. Fulghieri,[4,3] D. Gribble,[4,3] K. E. Ide,[1] X. James,[4,3] R. V. F. Janssens,[4,3] S. R. Johnson,[4,3] P. Koseoglou,[1] Krishichayan,[2,3] D. Savran,[6] and W. Tornow[2,3]

[1] *Technische Universität Darmstadt, Department of Physics, Institute for Nuclear Physics, 64289 Darmstadt, Germany*
[2] *Department of Physics, Duke University, Durham, North Carolina 27708-0308, USA*
[3] *Triangle Universities Nuclear Laboratory (TUNL), Duke University, Durham, North Carolina 27708, USA*
[4] *Department of Physics and Astronomy, University of North Carolina at Chapel Hill, North Carolina 27599-3255, USA*
[5] *Dipartimento di Fisica, Università degli Studi di Milano and Istituto Nazionale di Fisica Nucleare, Sezione di Milano, 20133 Milano, Italy*
[6] *GSI Helmholtzzentrum für Schwerionenforschung GmbH, 64291 Darmstadt, Germany*

observable sensitive to the structure of the GDR. Finally, this sensitivity of the γ-decay behavior in particular on small differences of the GDR resonance energies is shown to place strong constraints on the nuclear shape, here, as a show-case for the triaxiality of ^{154}Sm. The obtained shape parameters $\beta = 0.2926(26)$ and $\boxed{\gamma = 5.0(14)^\circ}$ agree well with recent configuration interaction calculations within the Monte Carlo Shell Model.

By including more basis vectors, we can get closer to exact solutions.

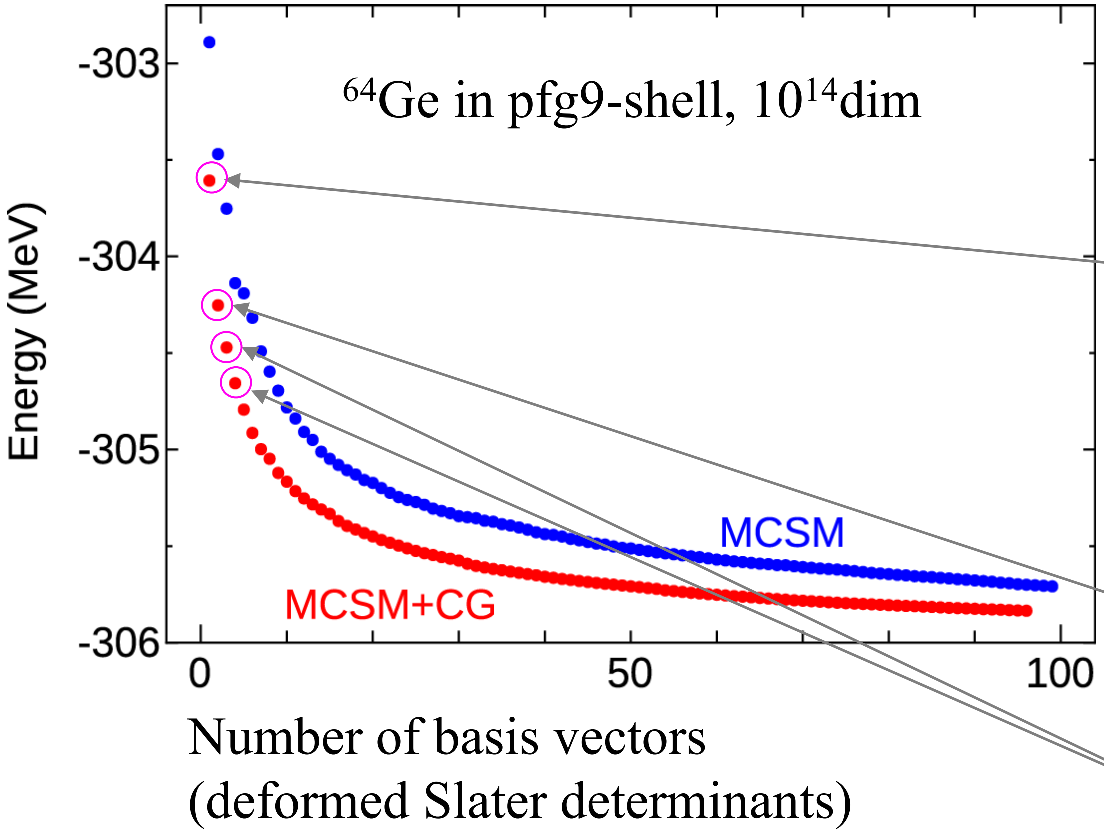

The MCSM calculation is carried out by successive search of basis vectors:

$$\left|\phi(D^{(n)})\right\rangle = \prod_{\alpha=1}^{N_p}\left(\sum_{i=1}^{N_{sp}} a_i^\dagger D_{i\alpha}^{(n)}\right)\left|-\right\rangle$$

The n=1 basis vector is fixed first by stochastic and variational searches for the most optimal $D^{(n=1)}$ matrix.
The initial guess for this search can be a mean-field solution, and we go beyond.

The n=2 basis vector is fixed next, under the presence of the n=1 basis vector.

The n=3, 4, … basis vectors are fixed likewise, driving the result closer to the exact solution.

physics

Physics 2022, 4, 258-285.
https://doi.org/10.3390/physics4010018

MDPI

Review

Emerging Concepts in Nuclear Structure Based on the Shell Model

Takaharu Otsuka [1,2,3]

Special Issue "The Nuclear Shell Model 70 Years after Its Advent: Achievements and Prospects"
edited by A. Gargano, G. De Gregorio and S. M. Lenzi

Shell evolution due to the monopole interaction

Type II shell evolution and shape coexistence

Triaxiality dominance in heavy nuclei as a consequence of the self-organization due to the monopole-quadrupole interplay ← *a bit more progress*

↔ traditional prolate dominance picture

New neutron dripline mechanism due to the monopole-quadrupole interplay, exemplified for F, Ne, Na and Mg isotopes

besides the traditional mechanism with single-particle nature

Alpha-clustering is not included

PES near the minimum: refined contour plots

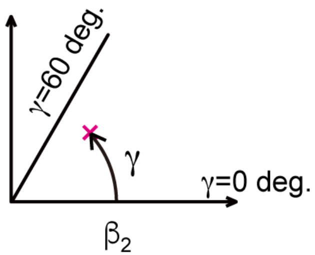

two most attractive monopole interactions $h_{11/2}$-$h_{9/2}$ and $g_{7/2}$-$i_{13/2}$ are weakened to average value

monopole interactions are replaced by constant SPEs assessed for spherical reference state (Monopole-Frozen)

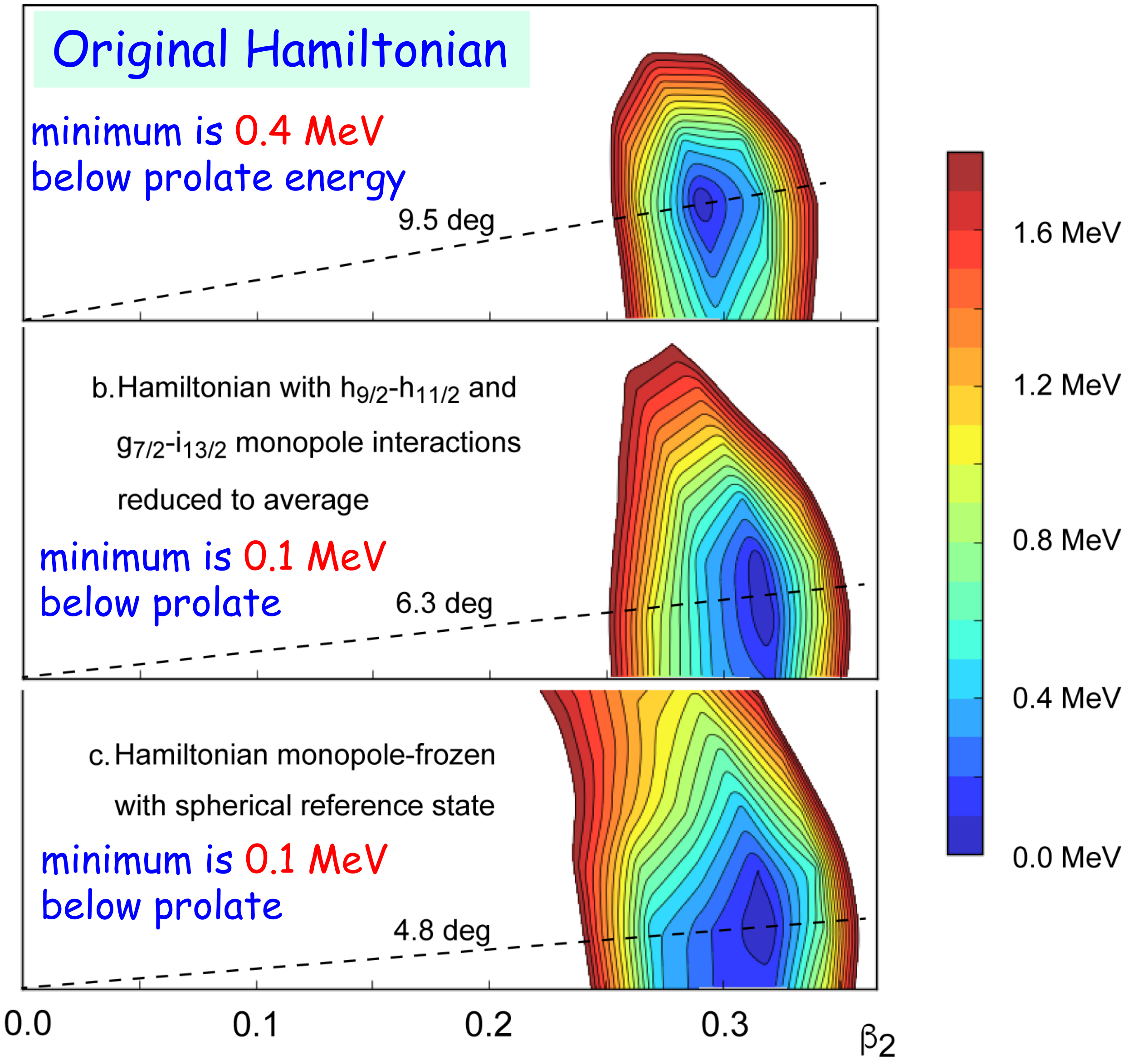

T plot of 0^+_1 state